國立交通大學

資訊工程系
碩士論文

應用於無線基頻應用之前端訊號處理研究

The Study of Front-End Signal Process for Wireless Baseband Applications

研究生：羅仕麟

指導教授：許騰尹 教授

中華民國九十三年七月

應用於無線基頻應用之前端訊號處理研究
The Study of Front-End Signal Process for Wireless Baseband Applications

研究生：羅仕麟　　Student : Shih-Lin Lo

指導教授：許騰尹　　Advisor : Terng-Yin Hsu

國立交通大學
資訊工程系
碩士論文

A Thesis
Submitted to Department of Computer Science and Information Engineering
College of Electrical Engineering and Computer Science
National Chiao Tung University
in partial Fulfillment of the Requirements
for the Degree of
Master
in

Computer Science and Information Engineering

July 2004

Hsinchu, Taiwan, Republic of China

中華民國九十三年七月

應用於無線基頻應用之前端訊號處理研究

學生：羅仕麟　　　　　　　　　　指導教授:許騰尹 博士

國立交通大學資訊工程學系　研究所碩士班

摘要

採用直接序列展頻的標準包含 802.11, 802.11b 以及 802.11g 等無線區域網路系統。無線通訊使用空氣當作介質，比有線通訊多了更多的不確定性，因此，無線通訊系統的封包裡一般都會定義 preamble 欄位作爲接收端封包偵測及同步之用。

而本論文提出一個有效率，應用於 802.11b 標準之自動增益控制、封包偵測及符元邊界決策。所提出的方法利用安置在每個封包之前的 preamble，在低訊號雜訊比、載波頻率偏移、多路徑衰減及路徑損失的通道時可以快速，正確的達到前端訊號處理的完成。而其中提出的自動增益控制演算法可在單一系統(直接序列展頻系統)以及雙系統(直接序列展頻系統和正交多工分頻系統)上使用。

爲了瞭解整個系統，我們使用 Matlab 建立了系統模擬平台。我們可以觀察系統中任一訊號的波形，並且可以得知通道中的非理想效應對整個系統或某些訊號有何影響。此平台更可以用來驗證我們所提出的演算法，本論文中也放了一些模擬結果圖，也驗證了演算法的成功。本論文中提到的 SNR 皆屬於進入 ADC 之前的 SNR。

The Study of Front-End Signal Process for Wireless Baseband Applications

Student: Shih-Lin Lo Advisor: Dr. Terng-Yin Hsu

Department of Computer Science and Information Engineering,
National Chiao Tung University

Abstract

Direct sequence spread spectrum (DSSS) technique is used in IEEE 802.11, 802.11b and 802.11g wireless LAN systems. Unlike the wire channel, wireless communication uses radio as its medium and has more uncertainty with it. Therefore, WLAN frame format generally contains preamble field for packet diction and synchronization.

In this thesis, an efficient automatic gain control (AGC), packet detection and symbol boundary decision for DSSS based WLAN defined in IEEE 802.11b had been proposed. The proposed methods enables a rapid and accurate front-end signal process even under very low SNR, carrier frequency offset multi-path fading and path loss channel by using preamble at the start of every frame. The proposed AGC algorithms could be used on single system (DSSS system) and dual system (DSSS system and OFDM system).

To get familiar with IEEE standards, simulation platforms were set up with Matlab mathematical software which let us have a chance to probe signals in every place inside the system and visual view of the channel effects. And with this system, our algorithms could be verified. Some simulation results were shown in this thesis, and the accomplishment of the proposed algorithms are also verified with these simulation results. These SNR that mentioned in this thesis belongs to the SNR that is before entering ADC.

Dedicate the thesis to my family and friends ……

Acknowledgements

I would like to express sincerely my gratitude to those people for their invaluable help during the past two years, stayed in Hsin-Chu. Especially, I want to express my deepest gratitude to my advisor Prof. Terng-Yin Hsu for his enthusiastic guidance and encouragement to overcome many difficulties throughout the research, and I give him and his family my best wish faithfully.

Also, I want to thank my ISIP group mates, Blues Yu(游瑞元), You-Hsien Lin(林祐賢), Ming-Fu Sun(孫明福), Jin-Hwa Guo(郭錦華), Ming-Yeh Wu(吳明曄), Ming-Feng Shen(沈明峰), Light Lin(林弘全), Chueh-An Tsai(蔡爵安), for their suggestions and great helps during my research. I would like to thank all members in ISIP laboratory for their plenty of fruitful assistance.

Finally, I give the greatest respect and love to my family and my girlfriend, Patty. I express my highest appreciation and dedicate the thesis to them for their assistance and attention during the most important stage in my life.

Contents

page

List of Figures *page*

List of Tables ***page***

CHAPTER 1

INTRODUCTION

With the advence of modern wireless communication techniques, there are more and more wireless communications systems play an increasingly important role in our daily life, like Wireless LAN(IEEE 802.11, 802.11b[1], 802.11a[2], 802.11g[3], UWB), Personal Communication System(GSM, PHS, 3G), Sensor Network or GPS, … etc. Despite what kind of the system is, the first problem is that "How to do the front-end signal process?" including Automatic Gain Control (AGC), packet detection and symbol boundary decision. For completely understanding the problem and solving it, the Direct Sequence Spreading Spectrum (DSSS) system is chosen to be my research area, so the IEEE 802.11b/g standard is used to build the demo platform to verify the proposed algorithms.

In the IEEE 802.11b standard, the PLCP preamble is used to do the front-end signal process, such as synchronization and channel estimation which use the Barker spreading code to eliminate non-ideal channel effects including Additive White Gaussian Noise (AWGN), distance path loss, Multipath fading, carrier frequency offset (CFO) and sampling clock offset (SCO). Not only IEEE 802.11b has included a preamble frame, but also many WLAN standards have done that. During this preamble, the front-end-signal process, such as timing synchronization, frequency synchronization and channel estimation must be done and some of channel effects have to be eliminated and compensated until the preamble finishes. Although the preamble formats are not the same in many WLAN standards, the problems that must be solved are all the same. If all these problems on IEEE 802.11b platform are solved, it could quickly find algorithms or solutions that solve these problems on other wireless platforms — IEEE 802.11a, IEEE 802.11g or UWB. In this thesis, the characteristics of both DSSS system and channel models would be described the information of PN spreading code during received preamble.

This thesis includes six chapters; where chapter 1 is the introduction DSSS system, and chapter 2 is the wireless signaling. Chapter 3 discusses the channel models and the current used simulation platform, and then chapter 4 discusses the front-end signal process methods in detail. In chapter 5 the performance PER and BER with Matlab simulation platform are shown. Finally, chapter 6 is the conclusions and future works for further research.

CHAPTER 2

WIRELESS SIGNALLING

2.1 Introduction

There are many restrictions of wireline networking such as not convenient to build wires between the transmitter and the receiver and wasted a lot of additional cost to build wires. Hence, radio or light are widely used to solve above problem, where several kinds of techniques based on radio or light to communicate or to transmit data, called Wireless Network. In Table 2-1 there is the summary of different specifications and standards.

Generally a lot of WLAN and WPAN systems use radio as medium to connect together, where many different standards are shown in [4]. The characteristics of DSSS technique would be introduced next.

Table 2-1 Medium and technique

Medium	Technique
Light	Infrared, Laser
Radio	802.11, 802.11b, 802.11a, 802.11g, UWB, Bluttooth, HomeRF, HiperLAN

2.2 Spreading technique

In 1997, the IEEE adopted IEEE std. 802.11-1997 where the first wireless LAN standard was proposed. This standard defines the media access control (MAC) and physical layers (PHY) for a LAN operation with wireless connectivity. There are two important kinds of spreading techniques, defined on IEEE 802.11; one is Frequency Hopping Spread Spectrum (FHSS) and the other one is DSSS.

a. Frequency Hopping Spread Spectrum (FHSS)

Frequency Hopping utilizes a set of narrow channels and "hops" through all of them in a predetermined sequence. For example, the 2.4 GHz frequency band is divided into 70 channels of 1 MHz each. Every 20 to 400 ms the system "hops" to a new channel following a predetermined cyclic pattern. The 802.11 Frequency Hopping Spread Spectrum (FHSS) PHY uses the 2.4 GHz radio frequency band, operating with at 1 or 2 Mbps data rate. Figure 2-1 is an example of FHSS.

b. Direct Sequence Spread Spectrum (DSSS)

The principle of Direct Sequence is to spread a signal on a larger frequency band by multiplexing it with a signature or code to minimize localized interference and background noise. To spread the signal, each bit is modulated by a code. In the receiver, the original signal is recovered by receiving the whole spread channel and demodulating with the same code used by the transmitter. The 802.11 Direct Sequence Spread Spectrum (DSSS) PHY also uses the 2.4 GHz radio frequency band and supports 1 or 2 Mbps data rate. The quantity of spreading code can be changed, the more spreading code can against more noise interference, and the lower spreading code can support more number of communications. Figure 2-2 is an example of DSSS.

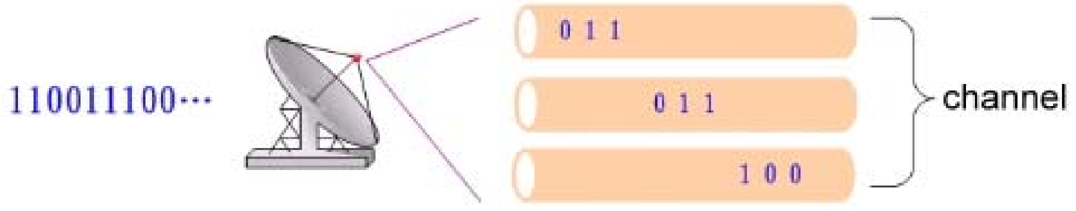

Figure 2-1 FHSS example

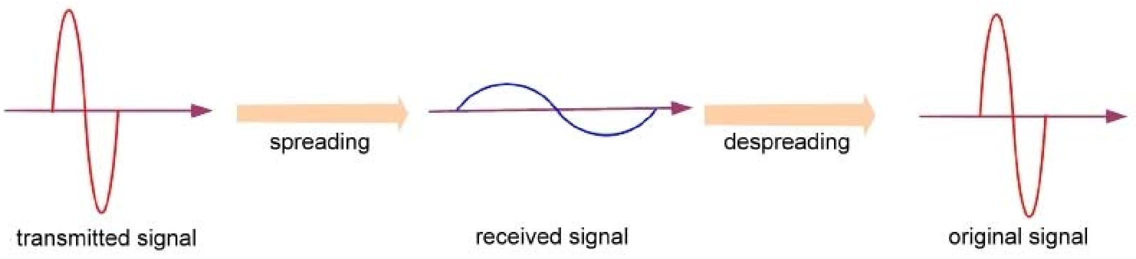

Figure 2-2 DSSS example

Table 2-2 DBPSK encoding table

Bit input	Phase change
0	0
1	π

2.3 DSSS-based IEEE 802.11

Assume that the original data is S(t) = 1 0 0 1 and the spreading code used in 802.11b is called Barker code is like bellow

B = [+1 -1 +1 +1 -1 +1 +1 +1 -1 -1 -1]……………………………………………..(2-1)

If the modulation type is Differential Binary Phase Shift Keying (DBPSK), then the original data after modulation would be $S_m(t)$. We can get DBPSK encoding flow from Table 2-2.

$$\theta_i = S(t) \bullet \pi + \theta_{i-1} \quad \text{...}\ldots\ldots(2\text{-}2)$$

$$S_m(t) = \sum_{i=1}^{n} e^{j\theta_i} \quad \ldots\ldots(2\text{-}3)$$

So the original S(t) after modulation is $S_m(t)$ is [-1 -1 -1 1].

Next $S_m(t)$ will be spreading with Baker code. The signal after spreading is

$$S_B(t) = S_m(t) \bullet B$$

$$= \sum_{i=1}^{n} e^{j\theta_i} \sum_k B_k \quad \ldots\ldots(2\text{-}4)$$

So the modulation signal $S_m(t)$ after spreading is

$S_B(t)$ = [-1 1 -1 -1 1 -1 -1 -1 1 1 1 -1 1 -1 -1 1 -1 -1 -1 1 1 1 -1 1 -1 -1 1 -1 -1 -1 1 1 1 1 -1 1 1 -1 1 1 1 -1 -1 -1]

and its waveform is shown in Figure 2-3.

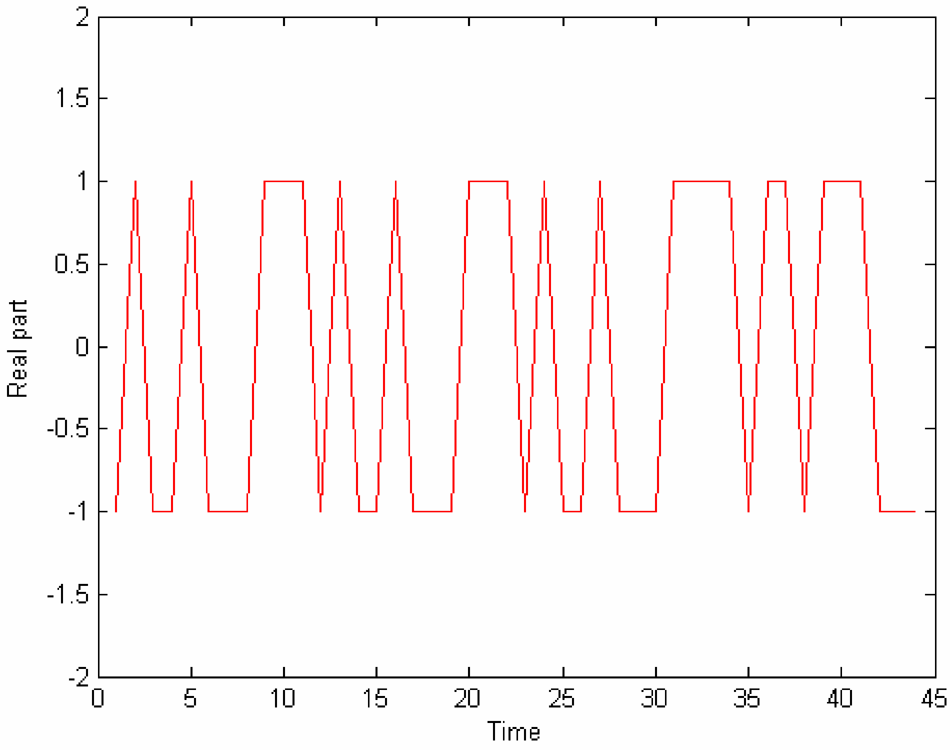

Figure 2-3 Waveform of Barker spreading output

2.3.1 Barker despreading

At the receiver, the received signal would be

$$R(t)=S_B(t)+n(t) \quad \ldots\ldots(2\text{-}5)$$

where n(t) is AWGN. Because the Barker code is a Psuede-Noise(PN) code, it has the characteristic as follows

$$B \bullet B=\sum_{k=1}^{11} B_k \bullet B_k \quad \ldots\ldots(2\text{-}6)$$

$$=\sum_{k=1}^{11} B_k^2$$

$$=\sum_{k=1}^{11} 1$$

$$=11$$

That is only when PN code is coherent to its self, the maximum value would appear. So if the received signal R(t) is transmitted to Barker correlator, the output is

$$
\begin{aligned}
C(t) &= (S_B(t)+n(t)) \bullet B \quad \text{...(2-7)} \\
&= [S_m(t) \bullet B + n(t)] \bullet B \\
&= S_m(t) \bullet B^2 + n(t) \bullet B \\
&= 11 \cdot S_m(t) + n(t) \bullet B
\end{aligned}
$$

Because AWGN n(t) has not spread with Barker code, n(t) will be spreading by Barker code and the signal $S_B(t)$ will be recovered by Baker code. Figure 2-4 shows real part of R(t) at Signal-to-Noise-Ratio(SNR) 0 dB and Figure 2-5 shows the output of Barker correlator. It could be found that almost every 11 cycles a maximum value appear would be appeared and AWGN n(t) seems does not affect the barker correlator badly. Figure 2-6 is power of barker correlator output. The formula is

$$
\begin{aligned}
Power &= \mathrm{Re}(C(t)) \bullet \mathrm{Re}(C(t)) + \mathrm{Im}(C(t)) \bullet \mathrm{Im}(C(t)) \quad \text{...(2-8)} \\
&= |C(t)|^2 \\
&\approx 121 \cdot |S_m(t)|^2 + 11 \cdot |n(t)|^2
\end{aligned}
$$

Compare Figure 2-4 and Figure 2-5, it could be found that if using the power level of barker correlator output as our information of any component, that will have more efficient than only using amplitude of barker correlator output. So the correlator output information can be used to do a lot of actions, such as AGC, AFC, etc in our system.

For an example, the received signal R(t) at receiver and SNR 0 dB is dispreading with Barker correlator. The point of maximum power value in one cycle could be known from Figure 2-5 and using the corresponding position to get the real part amplitude value from Figure 2-4. Then using these information of amplitude to get the corresponding phase information and then the differential phases of consecutive phase information could be used to do DBPSK decoding. For correctly decoding these differential phases, a more precisely decision rule is needed. Figure 2-7 and Figure 2-8 show the decision boundary of DBPSK and DQPSK respectively. These two decision rule are the most simple and efficient way to judge the differential phase and we can use the Q function formula to prove these decision rule is the best choice.

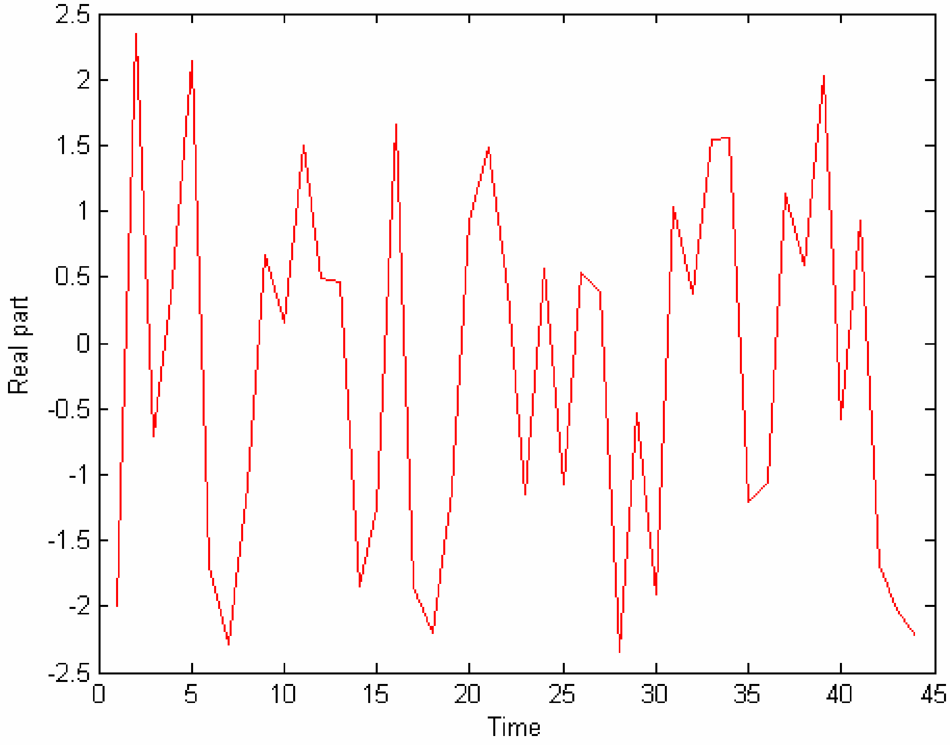

Figure 2-4 Real part of received signal R(t)

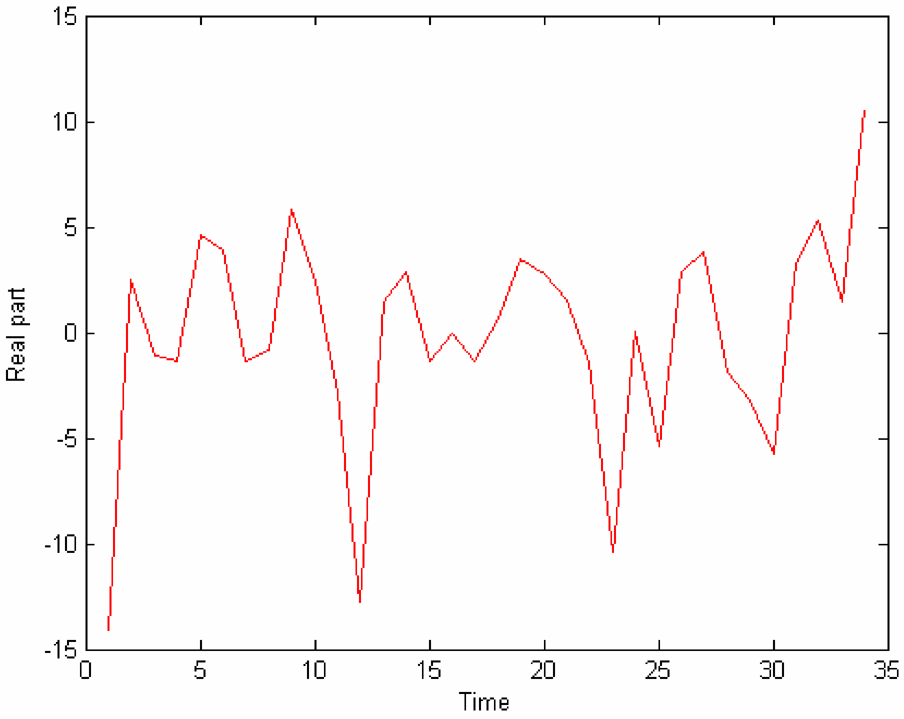

Figure 2-5 Real part of barker correlator output

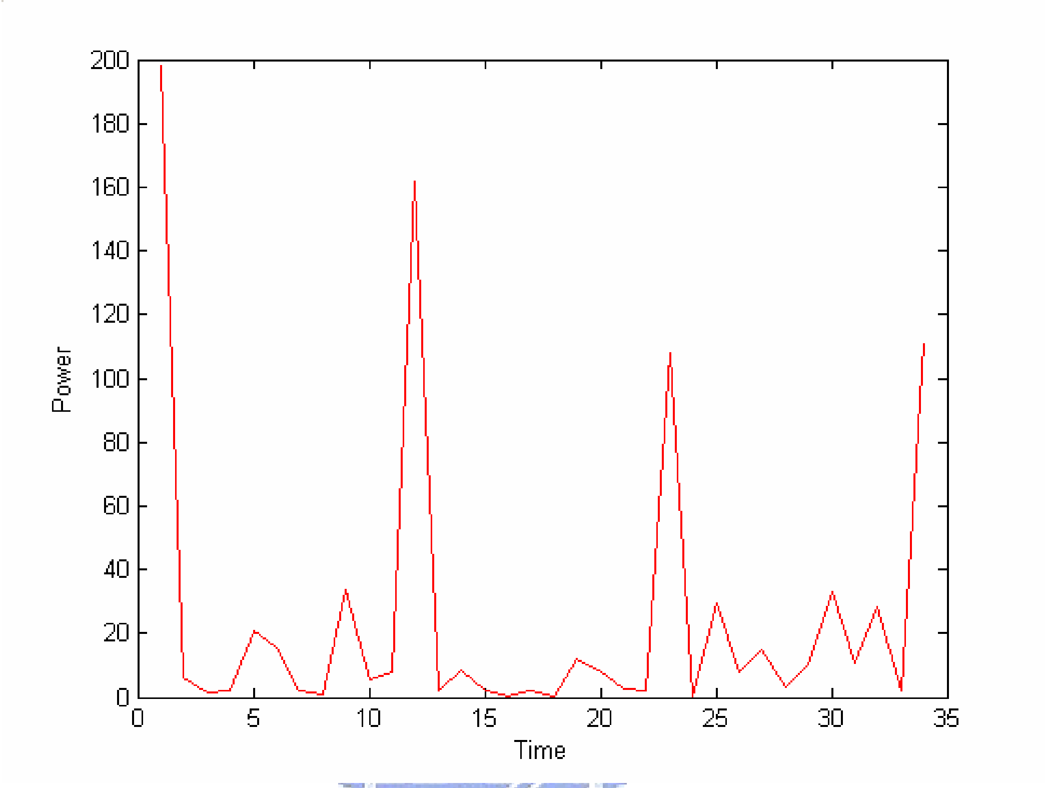

Figure 2-6 Power of barker correlator output

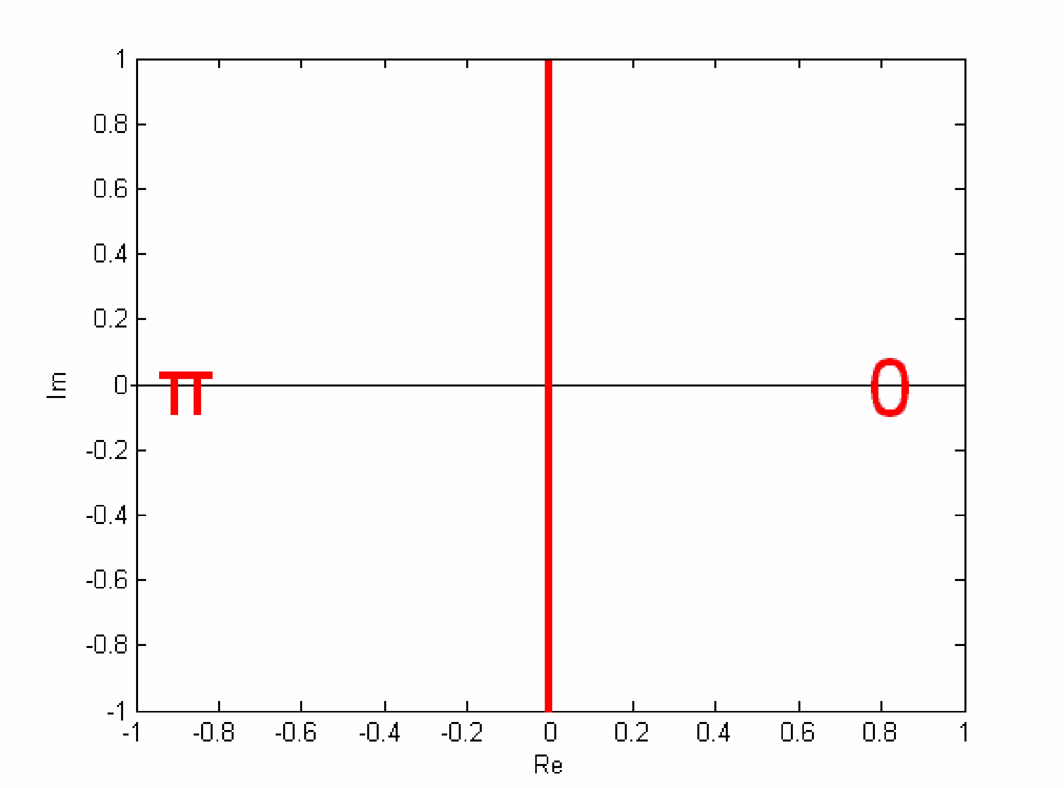

Figure 2-7 Decision boundary of DBPSK

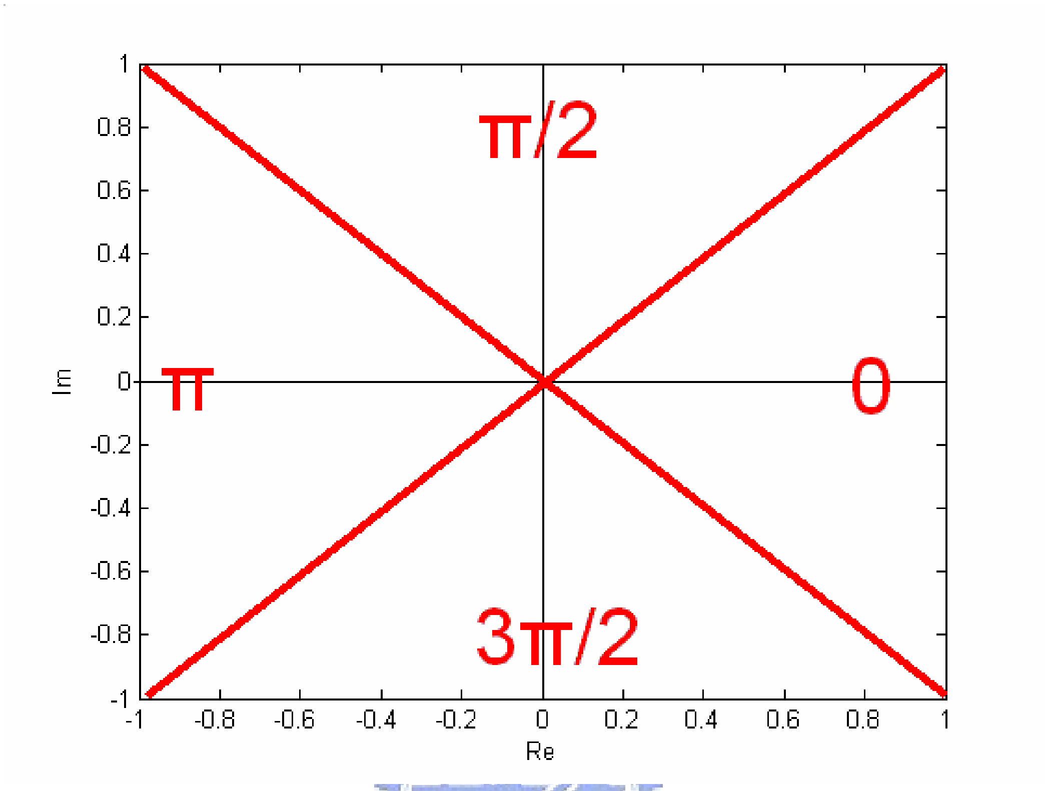

Figure 2-8 Decision boundary of DQPSK

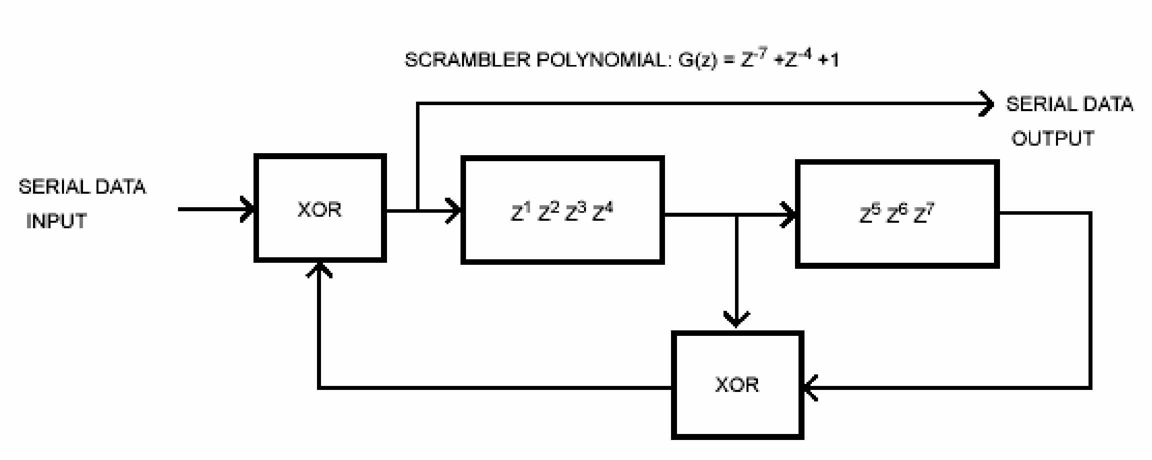

Figure 2-9 The architecture of scrambler

2.3.2 Scramble

Scrambling play an important role in many wireless communication systems, because it can suppress the dc effect on RF side. In 802.11b system, the architecture of scrambler is shown in Figure 2-9 and the initial state of register Z is [1 1 0 1 1 0 0].

In 802.11b system, scrambling is done before modulation and Barker spreading and after the preamble and data are combined.

2.3.3 CRC-16

CRC-16 is a very popular error check polynomial used in many network systems. In 802.11b system, only when CRC-16 filed is correcting it just can go on to decode the data. So the BER and PER calculation function will depend on whether CRC-16 filed is correcting or not. The CRC-16 polynomial is

$G(x) = X^{16} + X^{12} + X^{5} + 1$ …………………………………………………………..(2-9
)

And the architecture of CRC-16 is shown in Figure 2-10

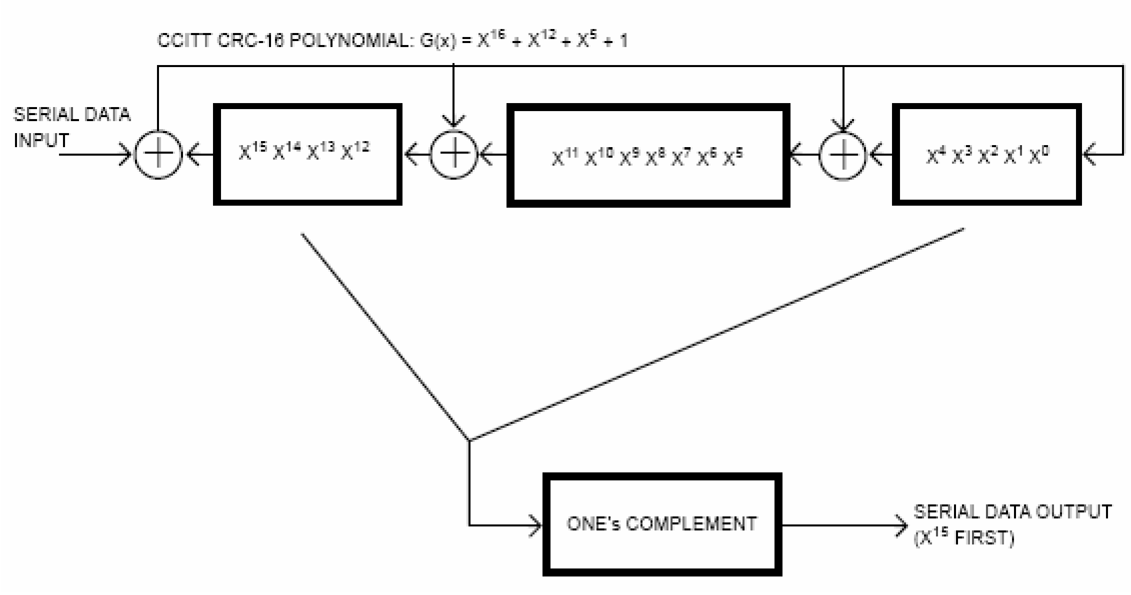
CCITT CRC-16 POLYNOMIAL: $G(x) = X^{16} + X^{12} + X^{5} + 1$
SERIAL DATA INPUT
$x^{15}\ x^{14}\ x^{13}\ x^{12}$
$x^{11}\ x^{10}\ x^{9}\ x^{8}\ x^{7}\ x^{6}\ x^{5}$
$x^{4}\ x^{3}\ x^{2}\ x^{1}\ x^{0}$
ONE's COMPLEMENT
SERIAL DATA OUTPUT
(X^{15} FIRST)

Figure 2-10 The architecture of CRC-16

2.3.4 Pulse shaping filter

There are restrictions of transmitting spectrum in many wireless systems. So these standards provide a transmit spectrum mask on their own. Figure 2-11 shows the transmit spectrum mask of 802.11b standard. To fit the transmit spectrum mask, we need a pulse shaping filter and raised-cosine filter is used in our system. The transfer function is

$$H(f)=\left\{\begin{array}{cc} 1 & for|f|<2W_o-W \\ \cos^2(\frac{\pi}{4}\frac{|f|+W-2W_o}{W-W_o}) & for 2W_o-W<|f|<W \\ 0 & for|f|>W \end{array}\right\} \text{.......................................(2-10)[5]}$$

where W is the absolute bandwidth and W_o = 1/2T represents the minimum Nyquist bandwidth for the rectangular spectrum. The corresponding impulse response is

$$h(t)=2W_o(\sin c2W_ot)\frac{\cos[2\pi(W-W_o)t]}{1-[4(W-W_o)t]^2} \text{..(2-11)[5]}$$

And Figure 2-12 shows the impulse response of raised cosine filter with different roll-off factors. Another advantage of using raised cosine filter is that signal through it can reduce Inter Symbol Interference(ISI) effect and without ISI effect our performance will increase 2 to 3 dB. Hence many wireless communication systems use the raised cosine filter in them to reduce ISI.

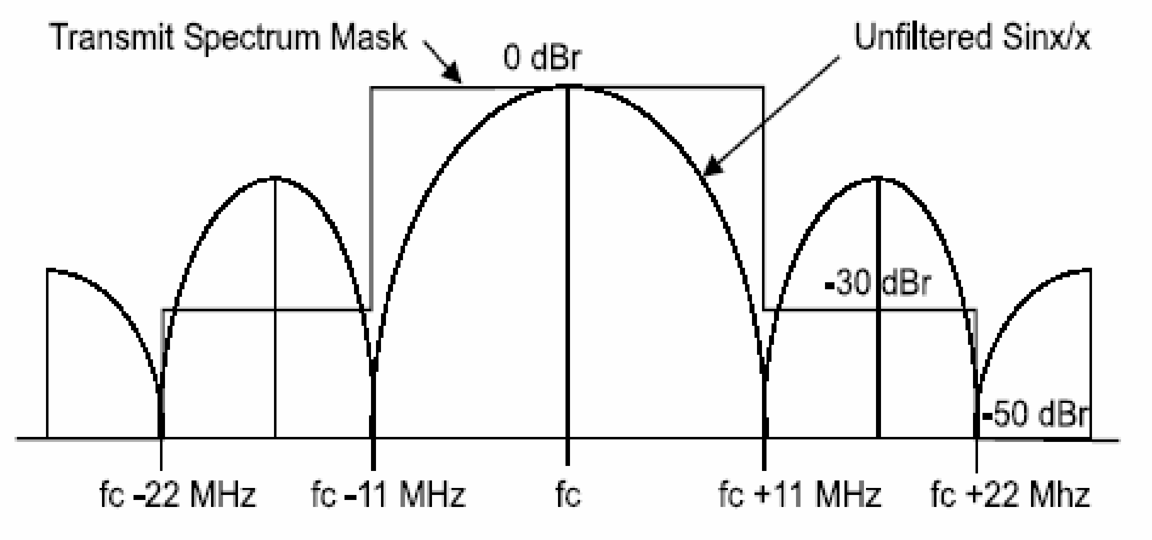

Figure 2-11 Transmit spectrum mask

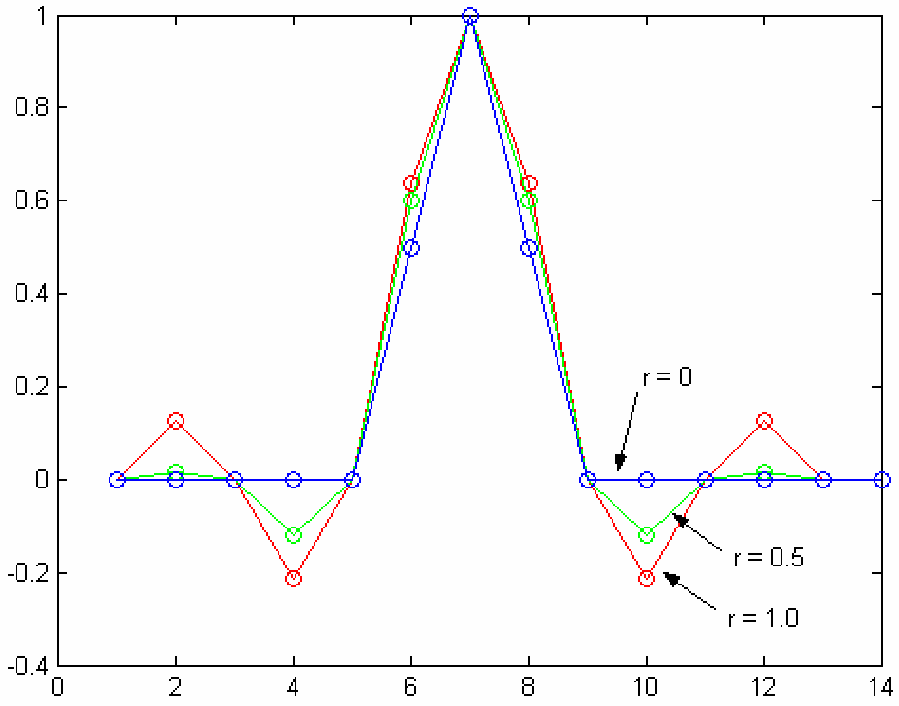

Figure 2-12 Impulse response of raised cosine filter with different roll-off factors

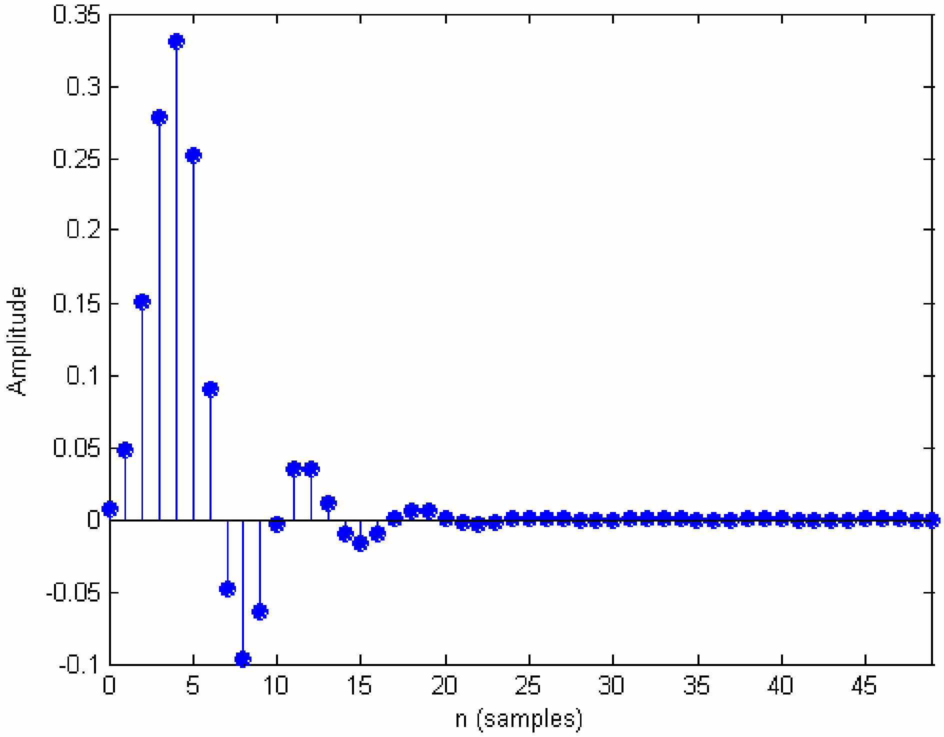

Figure 2-13 Impulse response of butter worth filter with 5-order tap

2.3.5 Low-pass filter

At the receiver, a digital low-pass filter is needed to filter the high frequency, wanted signal, such as butter worth filter. Because it is a digital filter, there is a finite order n in this digital filter design. Figure 2-13 is the impulse response of design of butter worth filter with 5-order tap.

In this section, each component is an important unit respectively where demo platform is based on above technique, architecture and performance evaluation to discuss in next chapter.

CHAPTER 3

CHANNEL MODEL

3.1 Channel effects

In any one wireless communications system, there are three important blocks that must be considered. The first is Transmitter (TX), the second is channel model and the last is Receiver (RX). Among these three blocks, the channel model is especially important than the others, because the channel effects truly reflect how the channel reacts in the real world. The two parts that composite the channel model is shown in Table 3-1, and Figure 3-1 shows a typical wireless communication system. It could be seen that one part of channel model is atmosphere model and the other is system inconsistency from Table 3-1. These channel effects would be introduced in this section.

Table 3-1 Two parts of channel model

Atmosphere model	System inconsistency
Path Loss	Carrier Frequency Offset
Multipath	Clock Drift
AWGN	

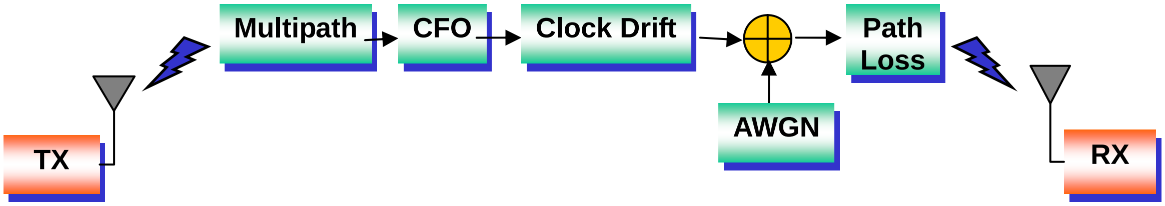

Figure 3-1 Typical wireless communication system

3.1.1 Path Loss

Because the signal power will decrease with the distance between TX and RX increasing, at the RX an amplifier that needed is called Variable Gain Amplifier (VGA) to amplify the received signal power, or the system will not detect any signal. Assume that the transmitted signal is s(t) and the received signal is r(t), then path loss effect can be modeled as

$$r(t) = s(t) \bullet path\_loss \tag{3-1}$$

where path_loss is a constant and its value is from 0 dB to -30 dB.

If the path loss effect is very crucial, the receiver will not detect any signal without an amplifier. However it can not be known that how much the path loss effect is, if there is not an AGC in a wireless communication system, the system will never get a steady signal, and even can not work any more. So the goal of AGC is to find the right path loss effect and justify the VGA gain to let the system can work under the situation of having steady signal.

3.1.2 Multipath

For a common system, the transmitted signal through a multipath fading channel can be written as

$$r(t) = \int_{-\infty}^{\infty} s(\tau) h(t,\tau) d\tau = s(t) \otimes h(t,\tau) \tag{3-2}$$

where t represents the time and τ represents the channel multipath delay for a fixed value of t. If the multipath channel is assumed to be a bandlimited bandpass channel and time invariant, then the channel impulse response may be simplified as

$$h_b(\tau) = \sum_{i=0}^{N-1} a_i \exp(j\theta_i) \delta(\tau - \tau_i) \tag{3-3}$$

where a_i and τ_i are the real amplitudes and excess delays, respectively, of i_{th} multipath component. The pahse term θ_i represents the phase shift due to free space propagation of the i_{th} multipath component, plus any additional phase shifts which are encountered in the channel. Any one who interested in multipath fading can reference [5].

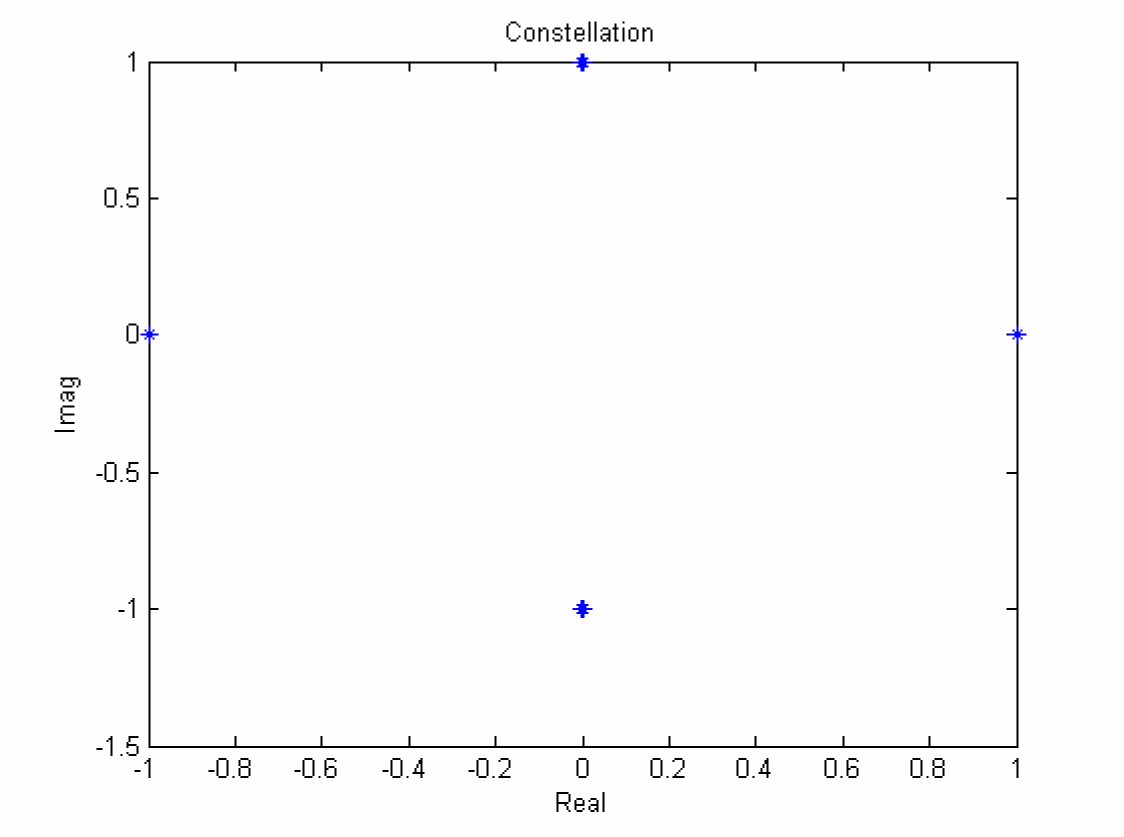

Figure 3-2 Constellation of transmitted signal

In this system, three public multipath model (SPW11b, SPW11a and IEEE Multipath) is used to simulate and some figures are shown to let everybody see how the multipath effects signal. Figure 3-2 shows the constellation of a transmitted signal, and the transmitted signal is modulated with DQPSK. Figure 3-3 shows three types of multipath impulse response and the transmitted signal through convolution with them.

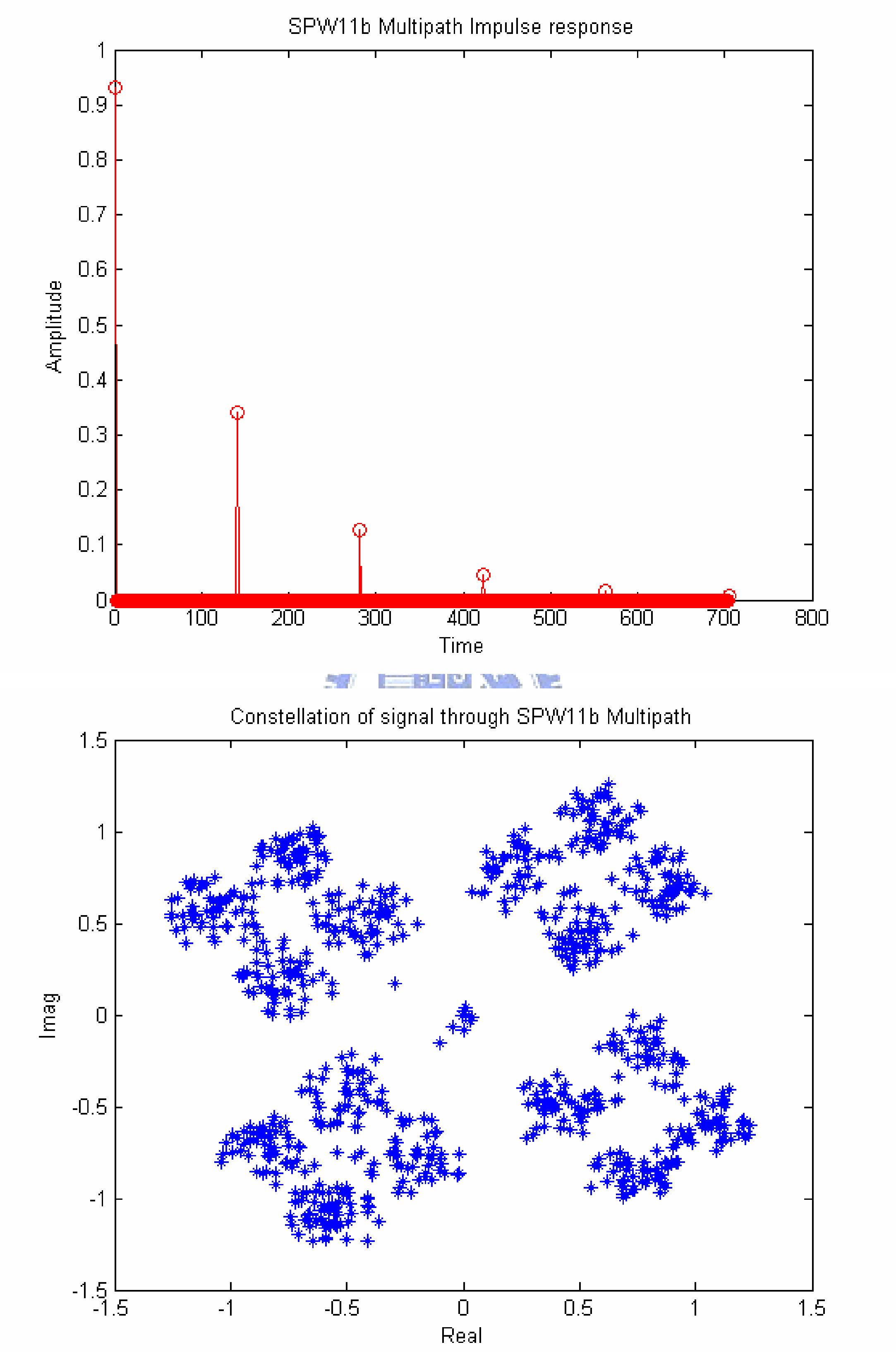

Figure 3-3 SPW11b multipath impulse response and constellation of signal

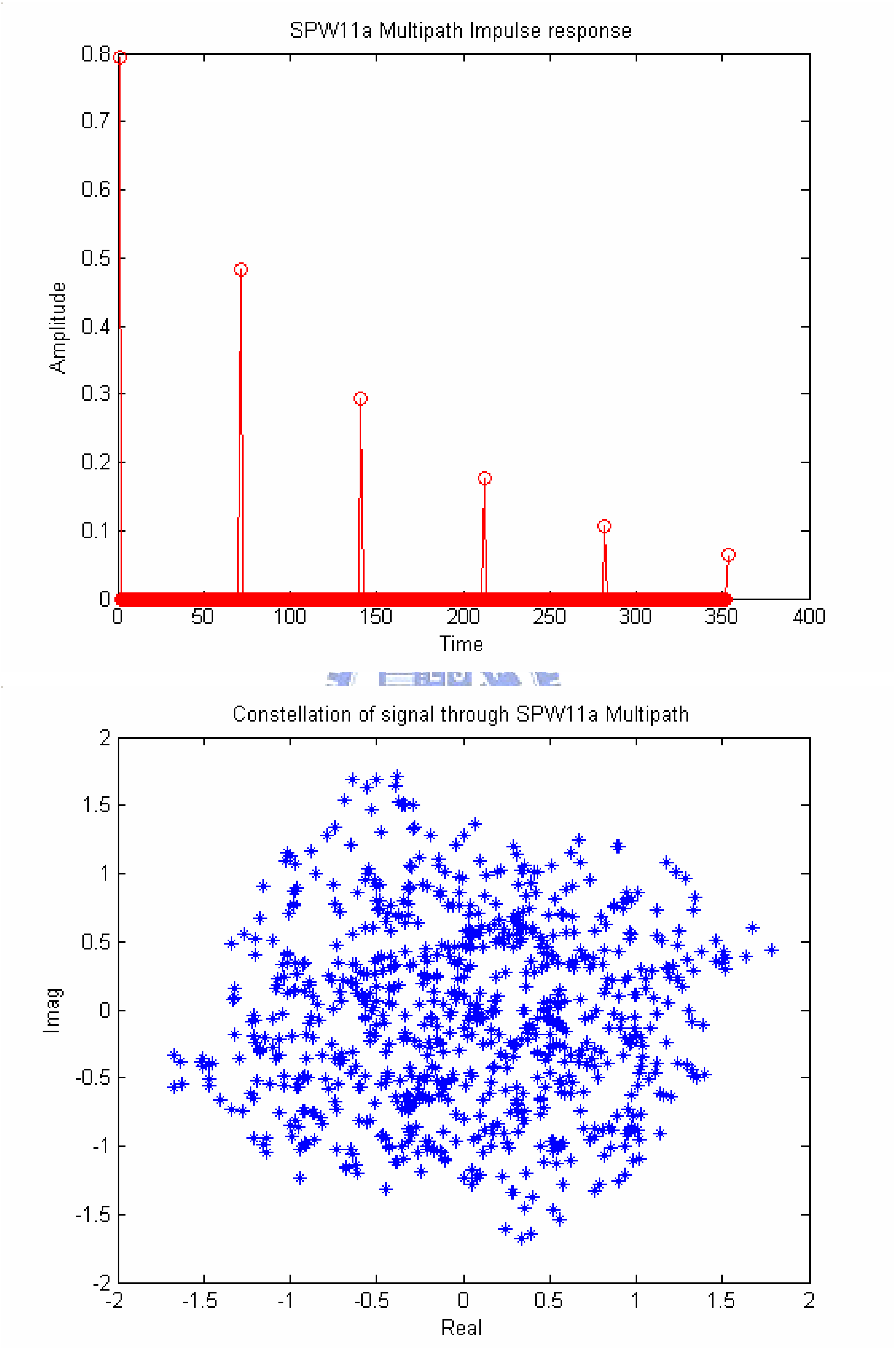

Figure 3-4 SPW11a multipath impulse response and constellation of signal

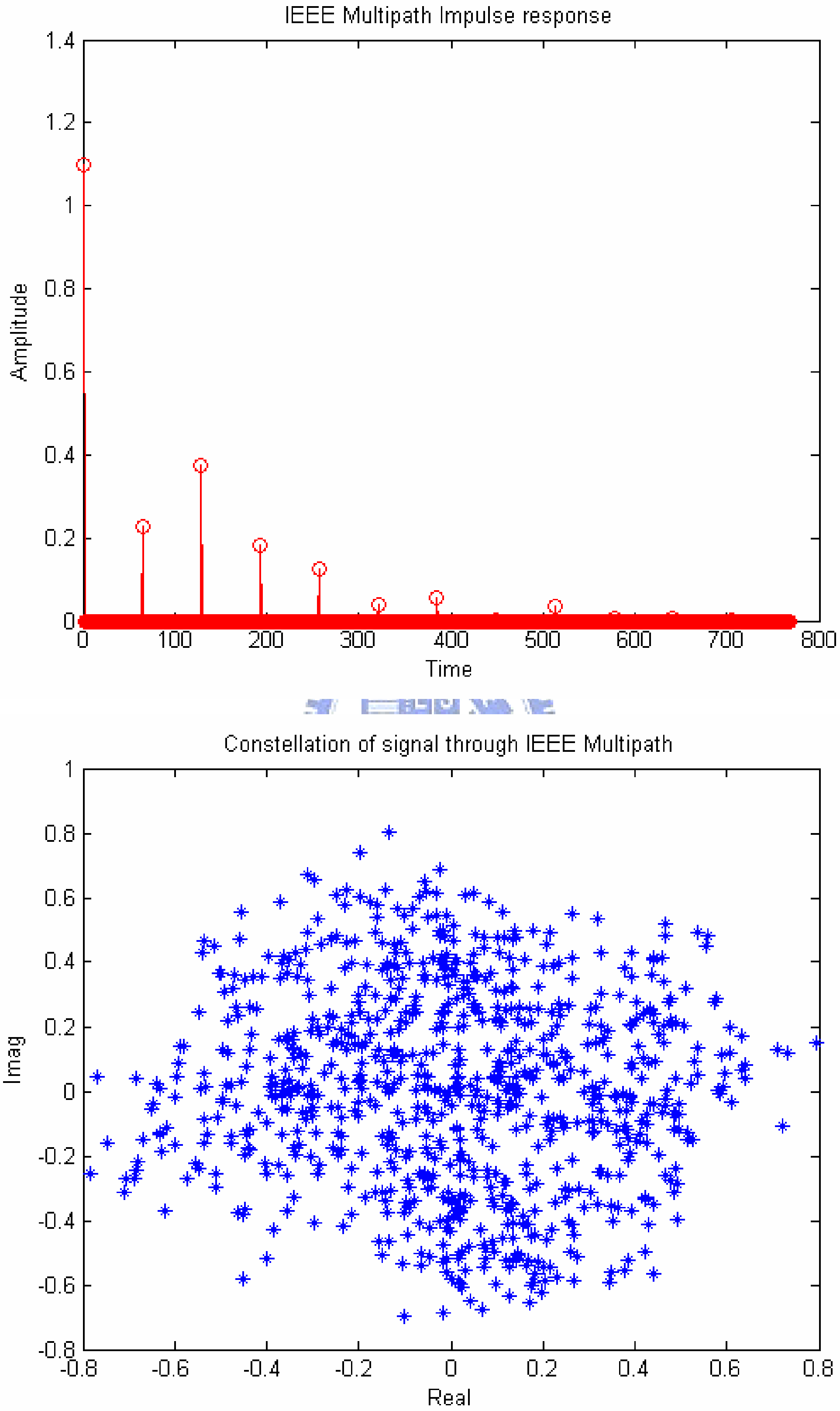

Figure 3-5 IEEE Multipath impulse response and constellation of signal

3.1.3 CFO

CFO is caused by the inconsistency between RF of TX and RX and its effect can be written as

$$r(t)=\sum_{n} s(t)\bullet\exp(j(2\pi\Delta ft+\theta)) \quad \text{...(3-4)}$$

where Δf and θ are the carrier frequency and carrier phase difference between TX and RX respectively. Figure 3-6 shows the constellation of signal through CFO=50 ppm and it shows that the CFO will cause the constellation of the transmitted signal become a circle, that means phase of the transmitted signal will rotate with time. a frequency synchronization algorithm will be proposed to eliminate this effect at chapter 4.

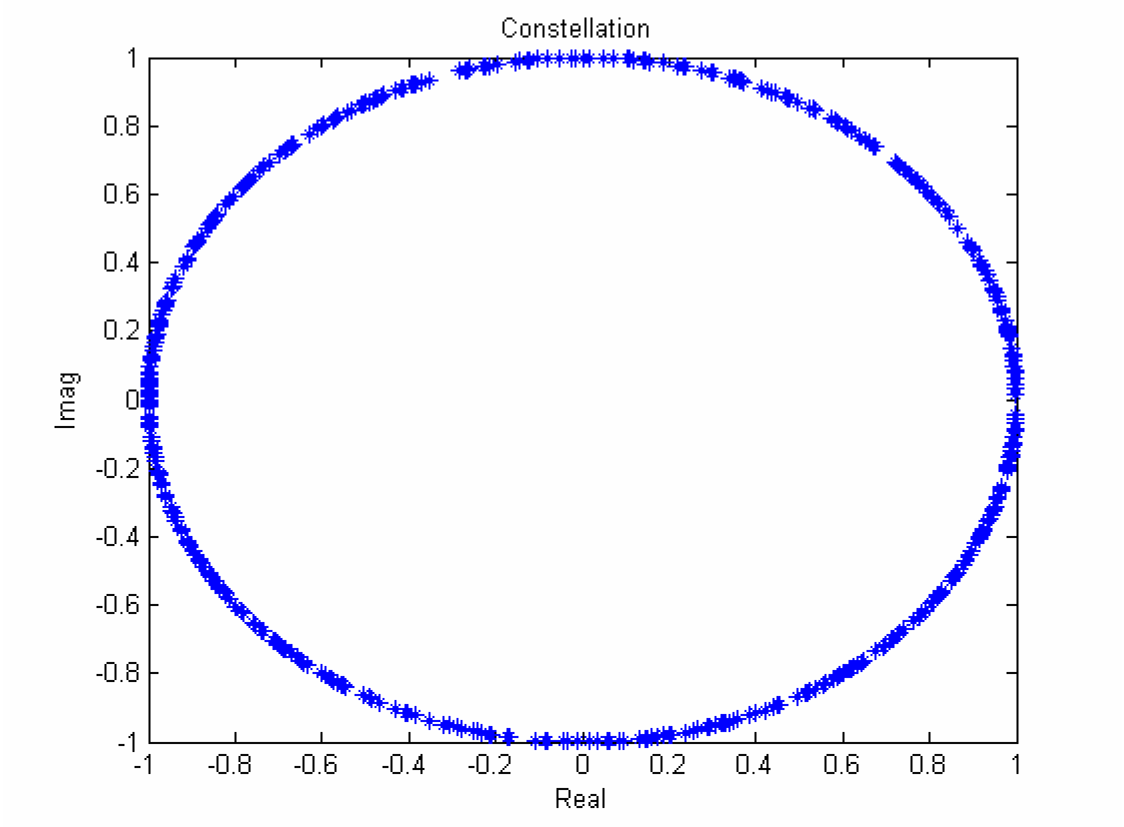

Figure 3-6 Constellation of signal through CFO=50 ppm

3.2 Matlab receiver platform architecture

There are three systems that are used for this thesis. Figurer 3-7 shows a DSSS system that is used to do the front-end signal process, frequency and timing synchronization. Figure 3-8 is a dual system constituted of DSSS system and Orthogonal Frequency Division Multiplexing (OFDM) system and this system is used to test the proposed dual system AGC algorithm. This AGC algorithm for single system (DSSS system) and dual system (DSSS system + OFDM system) is introduced in chapter 4. Figure 3-9 shows an complete 802.11b system that is used to calculate Bit-Error-Rate (BER) and Packet-Error-Rate (PER).

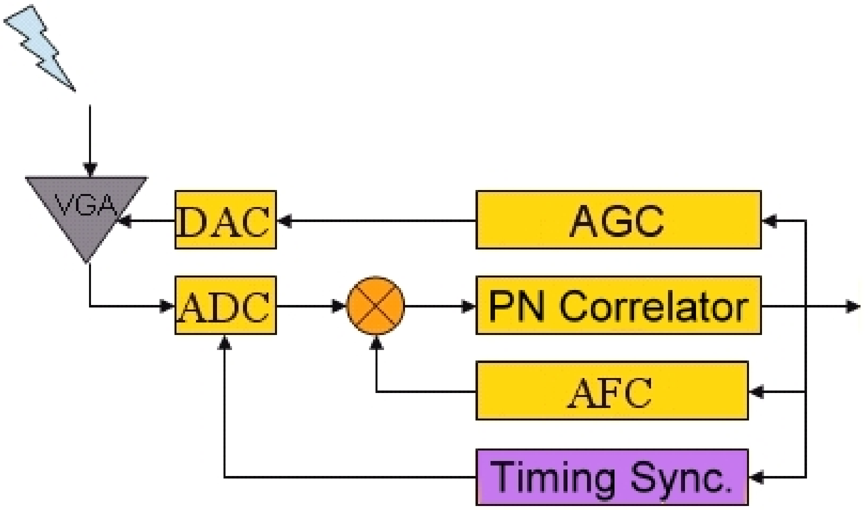

Figure 3-7 DSSS system architecture

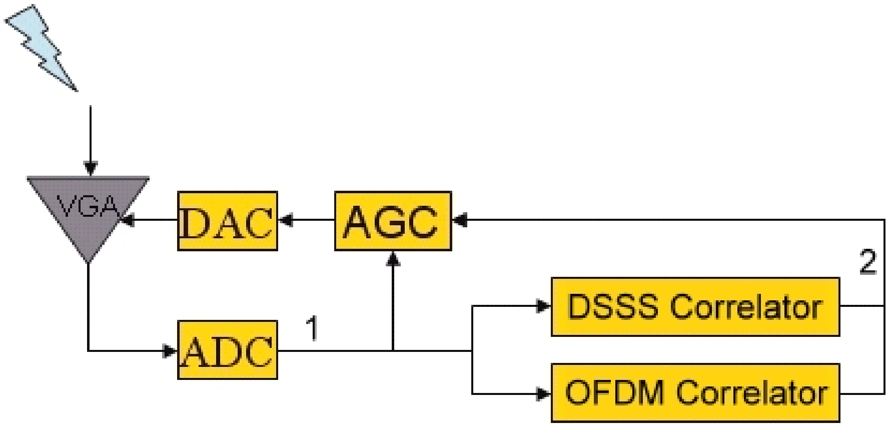

Figure 3-8 Dual system platform architecture

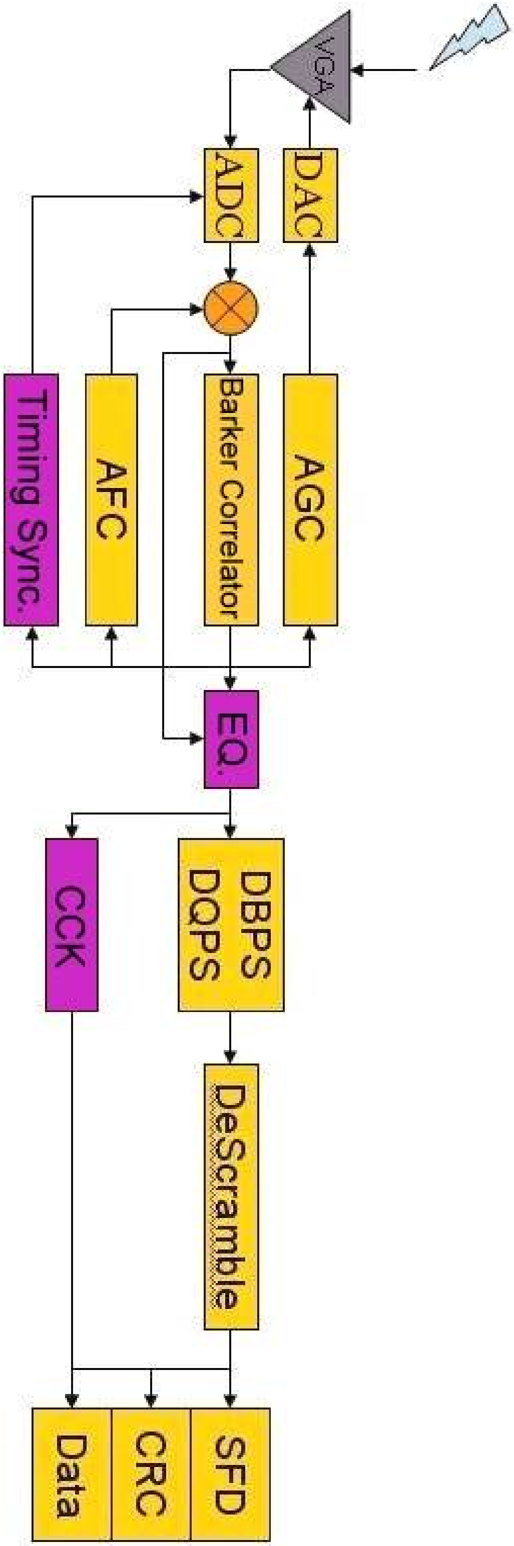

Figure 3-9 IEEE 802.11b platform architecture

CHAPTER 4

THE FRONT-END SIGNAL PROCESS

4.1 AGC algorithm

4.1.1 Single system

For any DSSS system, the PN correlator output is the most important information, hence in 802.11b system the Barker correlator output is used to do a lot of operation. So the proposed AGC algorithm is constructed based on the PN correlator output. Figure 4-1 shows the Barker correlator output in one symbol time. The peak means that the point having maximum correlator output power in one symbol time and its formula is

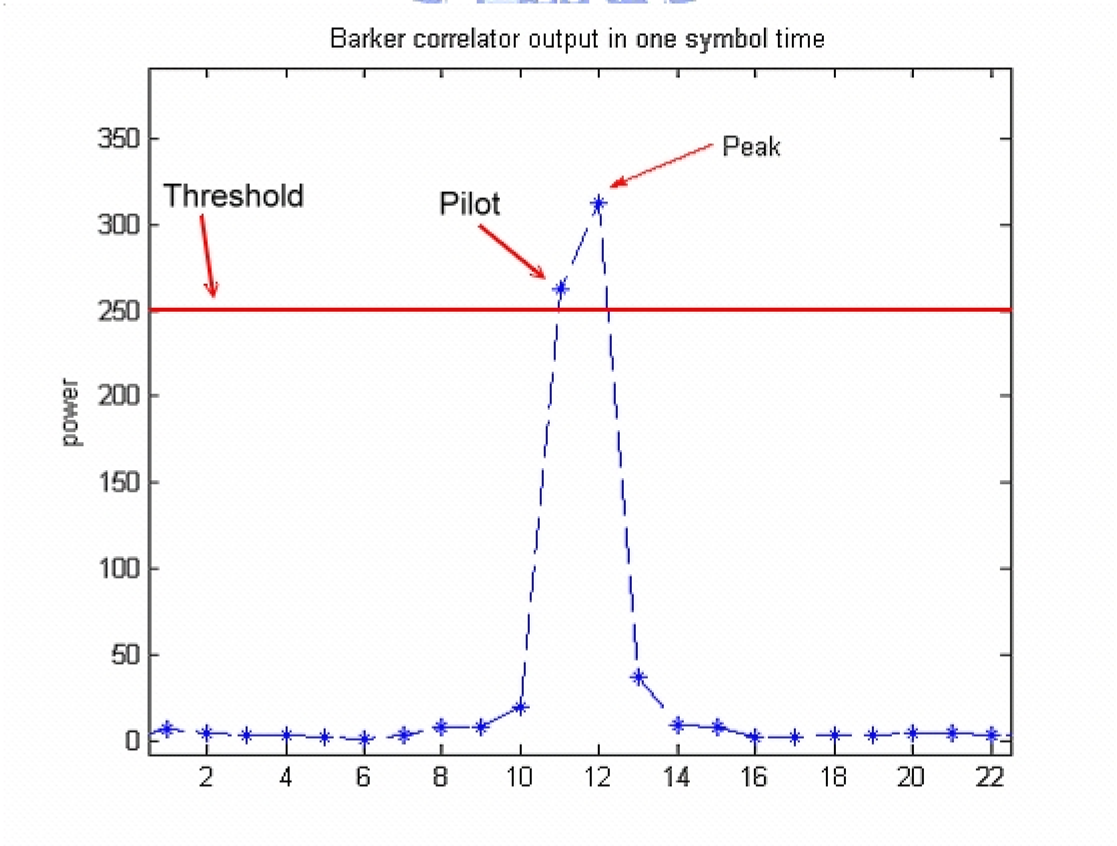

Figure 4-1 Barker correlator output during one symbol time

$$Peak\_power = Max(\mathrm{Re}(r(t-nT)\bullet B)^2 + \mathrm{Im}(r(t-nT)\bullet B)^2) \quad \ldots\ldots\ldots\ldots\ldots\ldots\ldots\ldots\ldots\text{(4-1)}$$

where T is symbol time duration and r(t) (the received signal) is

$$r(t) = (s(t) \otimes h(t) \bullet e^{j(2\pi\Delta ft+\theta)} + n(t)) \bullet path\_loss \quad \ldots\ldots\ldots\ldots\ldots\ldots\ldots\ldots\ldots\ldots\text{(4-2)}$$

where s(t) is the received signal, h(t) is multipath impulse response, Δf is CFO, θ is phase offset and n(t) is AWGN. The pilot is the first point that its correlator output power is over threshold in one symbol time, it is used to find the correct symbol boundary. The formula is

$$\begin{aligned} Pilot\_set &= \{\mathrm{Re}(r(t-nT)\bullet B)^2 + \mathrm{Im}(r(t-nT)\bullet B)^2 > threshold\} \quad \ldots\ldots\ldots\ldots\ldots\text{(4-3)} \\ &= \{i_1, i_2, \ldots. i_p\} \; and \; i_k \in \{i_1, i_2, \ldots. i_p\} \end{aligned}$$

$$where$$

$$p <= T/T_c \; and \; \mathrm{Re}(r(t-nT+i_kT_c)\bullet B)^2 + \mathrm{Im}(r(t-nT+i_kT_c)\bullet B)^2 > threshold$$

Pilot_set is a set of point that correlator output power are over threshold and pilot is the point that time is smallest in the pilot_set, that means pilot is the first point that its power value is over threshold during one symbol time. In real world, initially it could not be known that how much the path loss effect is, so the AGC set VGA gain at maximum for never losing any signal whatever the received signal is noise or a packet. Next (4-4) is used to calculate next VGA gain until the packet is coming.

$$G' = G - 10\bullet\log_{10}(\frac{M}{D}) \quad \ldots\ldots\ldots\ldots\ldots\ldots\ldots\ldots\ldots\ldots\ldots\text{(4-4)}$$

where G and G’ are current VGA gain and next VGA gain respectively. M is the measured barker correlator output and D is the desired barker correlator output. At here, two different kinds of barker correlator output are used. One is peak power and another is average correlator power, so these can be formulated as (4-5) and (4-6)

$$\begin{aligned} G' &= G - 10\bullet\log_{10}(\frac{Peak\_power}{D\_peak}) \quad \ldots\ldots\ldots\ldots\ldots\ldots\ldots\ldots\ldots\ldots\text{(4-5)} \\ &= G - 10\bullet\log_{10}(\frac{Max(\mathrm{Re}(r(t-nT)\bullet B)^2 + \mathrm{Im}(r(t-nT)\bullet B)^2)}{D\_peak}) \end{aligned}$$

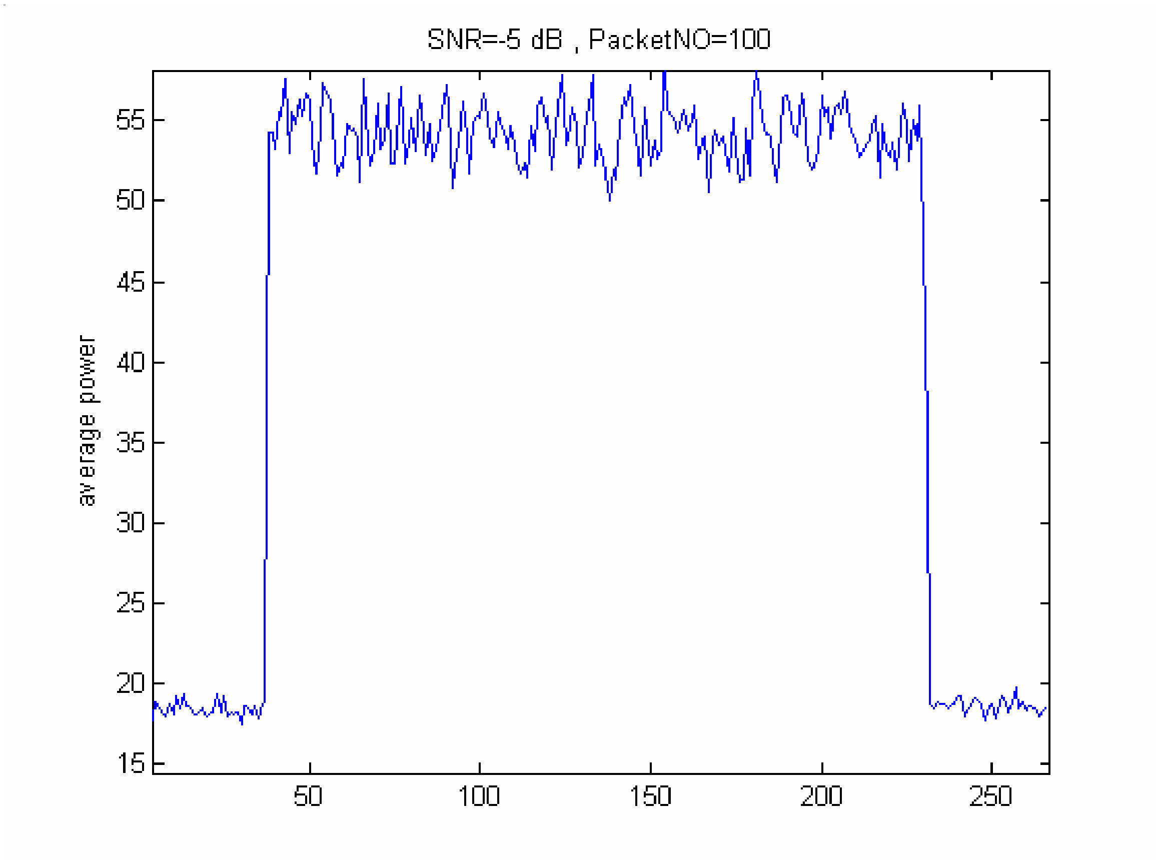

Figure 4-2 Average power of barker correlator output of 100 packets

$$G' = G - 10 \bullet \log_{10}\left(\frac{\dfrac{Sum(correlator\_output\_power)}{k}}{D\_avg}\right) \ldots\ldots\ldots\ldots\ldots\ldots\ldots\ldots\ldots(4\text{-}6)$$

$$= G - 10 \bullet \log_{10}\left(\frac{\dfrac{Sum(\mathrm{Re}(r(t-nT)\bullet B)^2 + \mathrm{Im}(r(t-nT)\bullet B)^2)}{k}}{D\_avg}\right)$$

where k is the number of chips in one symbol time and D_peak and D_avg are the desired peak power and desired average power respectively. Figure 4-2 shows the average barker correlator output of 100 packets with AWGN SNR=-5dB in front and end. It could know that the average power of noise and packets have their steady power respectively. Figure 4-3 shows the AGC state diagram for single system – DSSS system. Figure 4-4 shows how AGC justify the VGA gain versus time according to peak power and average power. If AGC use average power to justify VGA gain, the VGA gain will not change so rapidly and highly than using peak power. So the average power is used to justify VGA gain at AGC acquisition state. Figure 4-5 shows the situation of the received signal pass through VGA with AGC working and it could see that the relationship between figure 4-4 and figure 4-5. When detecting that packet comes, AGC will jump to the tracking state, and in tracking state AGC just use peak power to justify VGA gain and will calculate the next VGA gain after more symbol time than acquisition state. Figure 4-6 shows the Root-Mean-Square-Error(RMSE) at four kinds of environment-no multipath, SPW11b, SPW11a and IEEE Multipath from SNR -5dB to 10 dB. Next, how to detect whether a packet comes or not will be introduced.

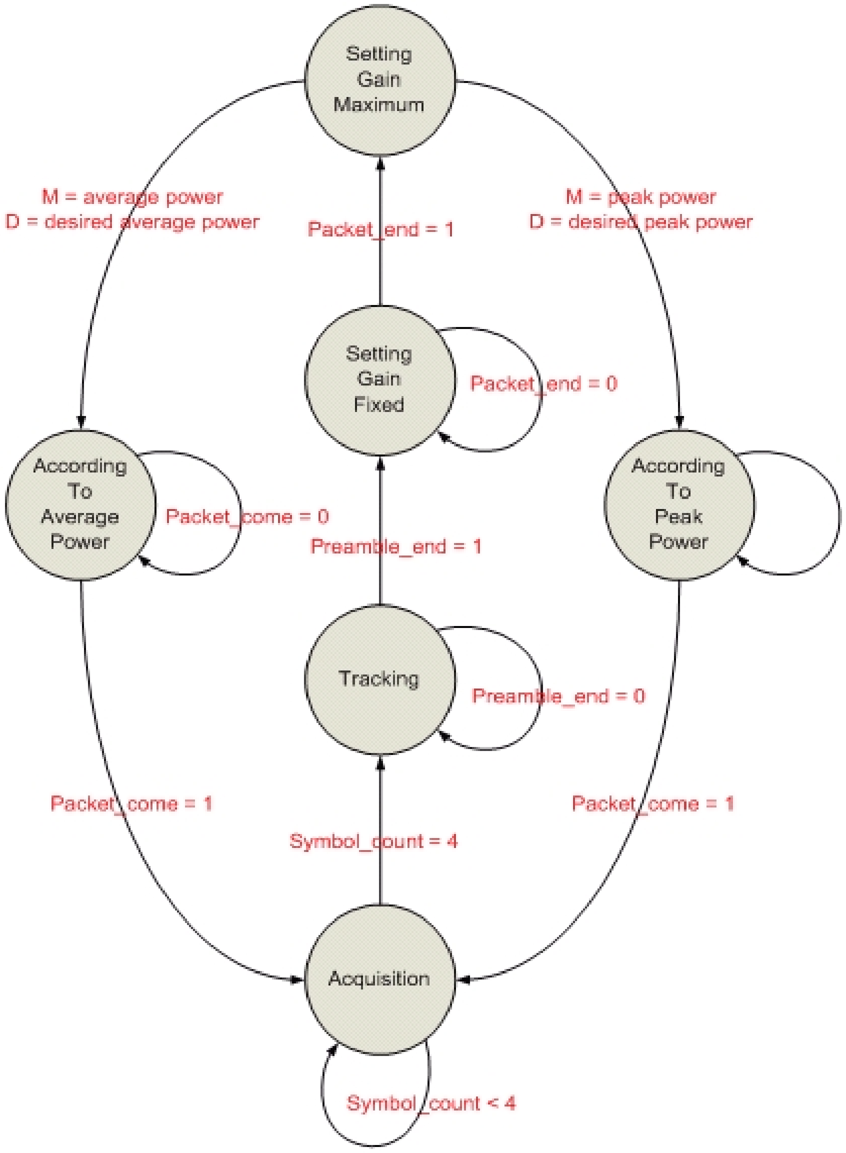

Figure 4-3 AGC state diagram for single system

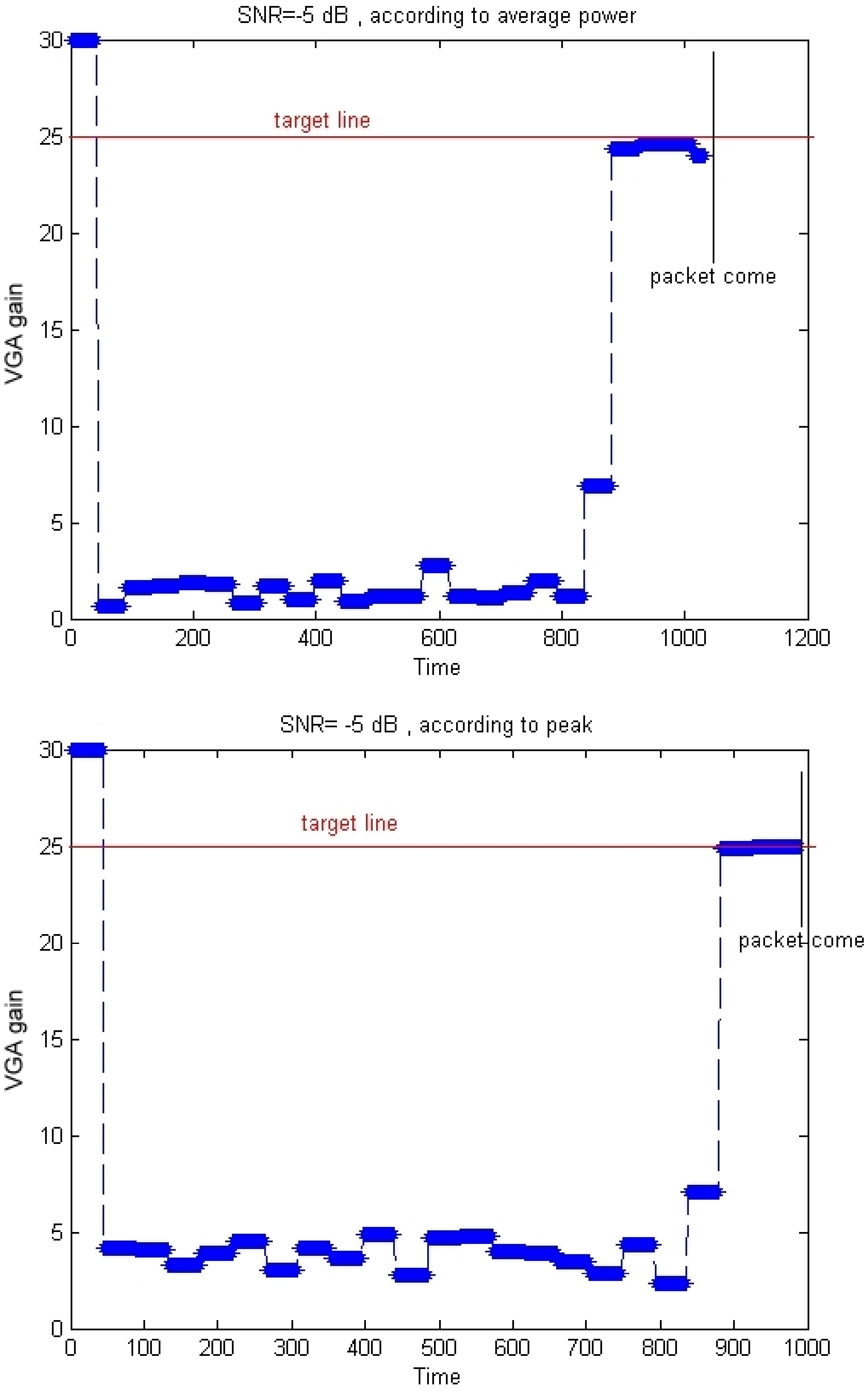

Figure 4-4 VGA gain adjustment at time domain

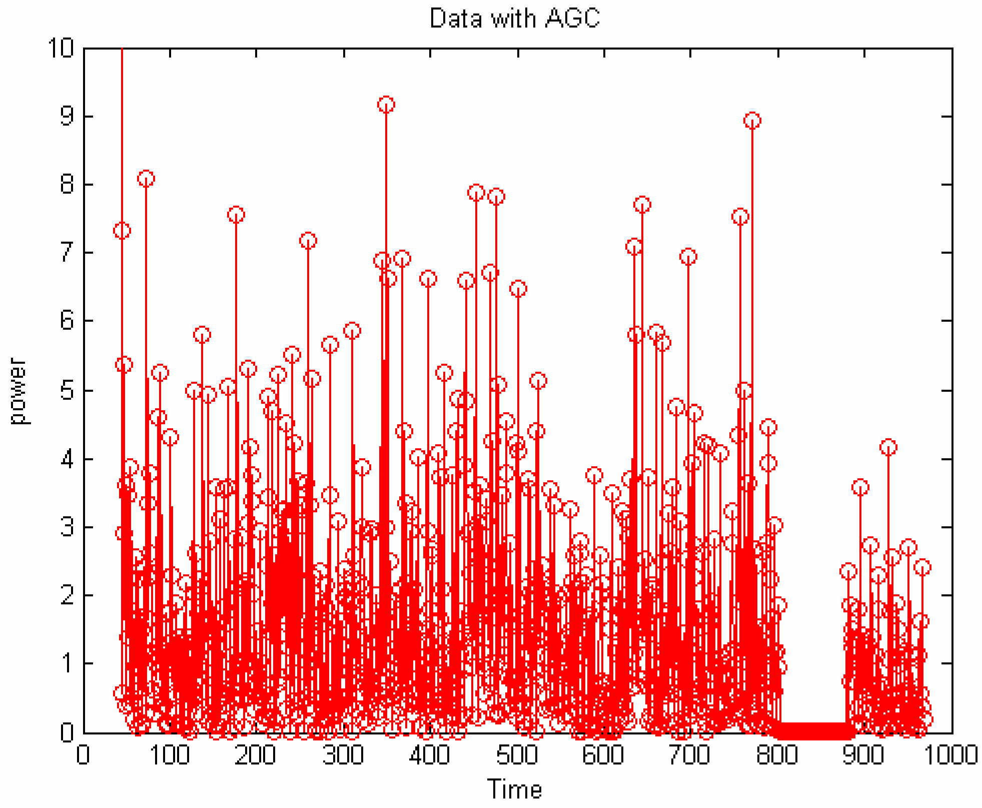

Figure 4-5 The received signal when AGC is on

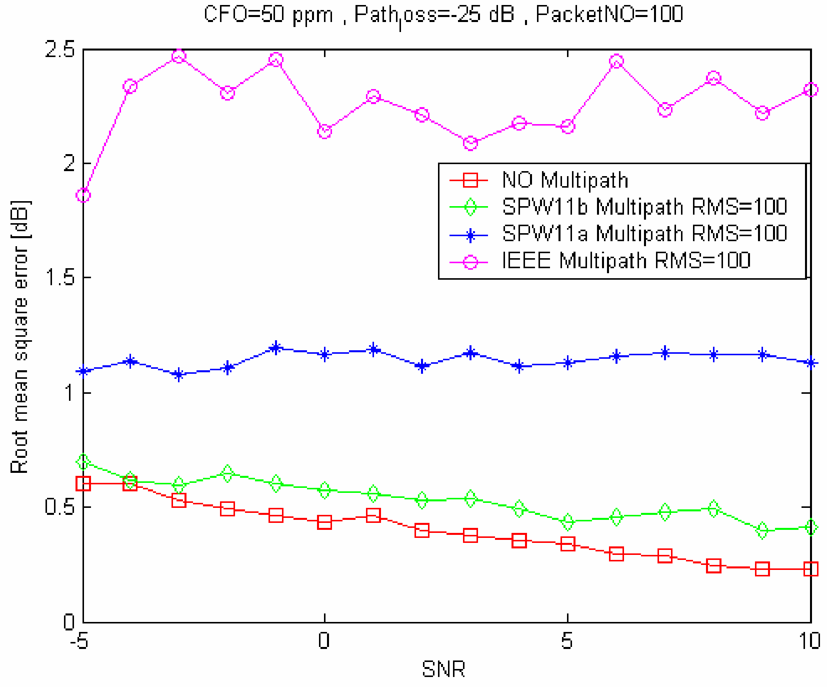

Figure 4-6 RMSE with none and three different kinds of multipath fading

4.1.2 Dual system

In a dual system, the critical issue is that the received signal must be quickly identified whether it belongs to which kind of system. So the dual system AGC algorithm is proposed based on this reason.

4.1.2.1 According to ADC sampling power

Initially, the received signal power must be adjusted at a suitable level, because the received signal could not be over the detecting range of ADC, the real packet information will be truncated by ADC and cause the situation that correlator could not clearly produce correct result. For quickly justifying the VGA gain, the ADC sampling point power is used by AGC and the formula is

$$Samp\_power = \sum_{k=1}^{N} \mathrm{Re}(r(t-nT+kT_c))^2 + \mathrm{Im}(r(t-nT+kT_c))^2 \quad \ldots\ldots\ldots\ldots\ldots\ldots\ldots\ldots(4\text{-}7)$$

where T_c is the chip time during one symbol time, N is the number of chips in one symbol time which equals T/T_c. Then the next VGA gain is calculated according to

$$G' = G - 10 \bullet \log_{10}\left(\frac{Samp\_power}{D\_samp}\right) \quad \ldots\ldots\ldots\ldots\ldots\ldots\ldots\ldots\ldots\ldots\ldots\ldots\ldots\ldots\ldots\ldots(4\text{-}8)$$

$$= G - 10 \bullet \log_{10}\left(\frac{\sum_{k=1}^{N} \mathrm{Re}(r(t-nT+kT_c))^2 + \mathrm{Im}(r(t-nT+kT_c))^2}{D\_samp}\right)$$

where D_samp is the desired sampling point power.

The advantage of using sampling point power is that the VGA gain can quickly be adjusted at a acceptable level, but the disadvantage is the VGA gain will easily be affected by AWGN, so the VGA gain will not be so stable. Based on this reason, once the packet type has been identified, the AGC state will change to tracking state to do more precise VGA gain adjustment. In the tracing state, the AGC will adjust according to the peak power of correlator output, hence the packet type has been known. Figure 4-7 shows the AGC state diagram of proposed dual system AGC algorithm. Compared with Figure

4-6, the only difference is that only at the packet detection state of AGC. The difference of acquisition state and tracking state is that the number of accumulating the peak power of correlator output, because before the end of preamble a more quickly estimating the VGA gain is needed based on the reason of reacting with quickly changeable channel and support the all synchronization components a stable without affecting by channel. The preamble filed is very important because all information about data is in it and all synchronization mechanism must be done before the end of preamble, so supporting a more quickly reacting and stable VGA gain is needed.

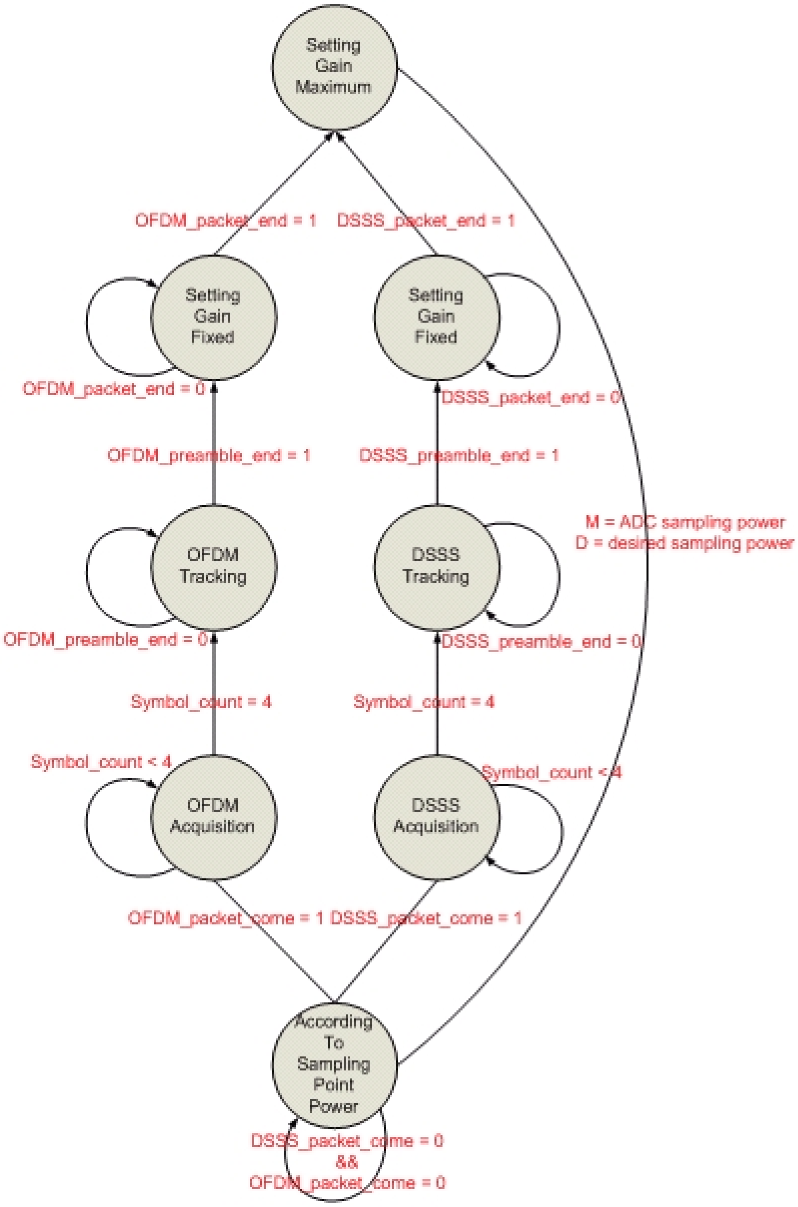

Figure 4-7 AGC state diagram for dual system

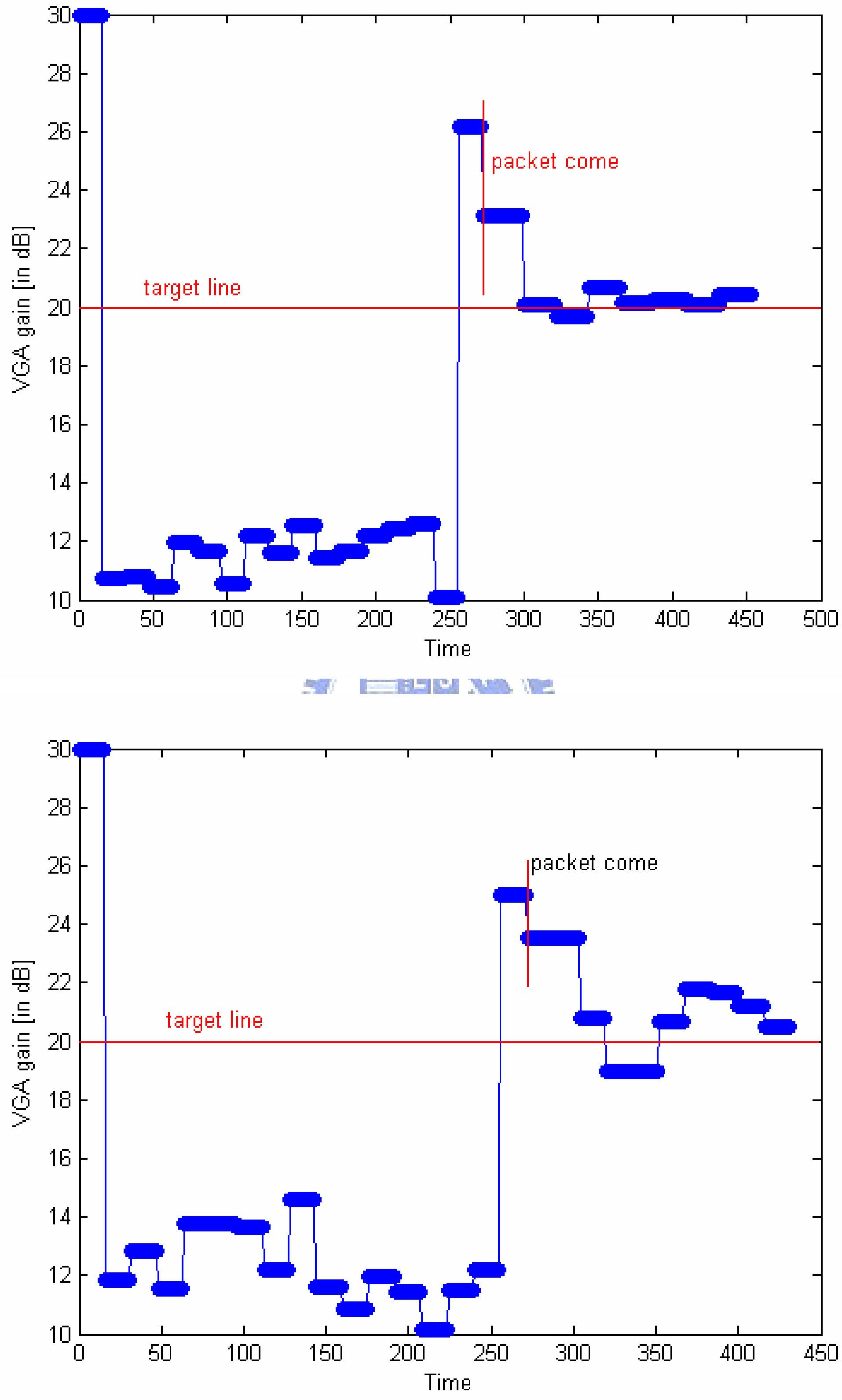

Figure 4-8 VGA gain adjustment at time domain

The VGA gain adjustment of dual system at time domain is shown in Figure 4-8. The up side is the situation of transmitting the DSSS type packet and the bottom side is the situation of transmitting the OFDM type packet. The VGA gain of transmitting OFDM type packet seems not so ideal, because the OFDM system is not my major research area, the characteristic of OFDM correlator has not been familiar with me. So, the study of characteristic of OFDM correlator is one of my future works.

4.1.2.2 According to correlator output average power

In this proposed method, the sum of correlator output average power of DSSS and OFDM is used. However, this method for dual system is a little different from the previous proposed method for single system. Because for quickly identifying what type of a packet is, we must let the buffer that saving data for correlating without be cleared. In the proposed method for single system, the buffer that saving data for correlating is cleared and we must waste a symbol time for getting the correct correlator output power. Because the preamble length of the DSSS system that is chosen is long enough to wait until that the buffer is cleared. Although the proposed method could quickly identify the packet type, the hardware cost will be higher than the method without clearing the buffer. The block diagram of this proposed method is shown in Figure 4-9.

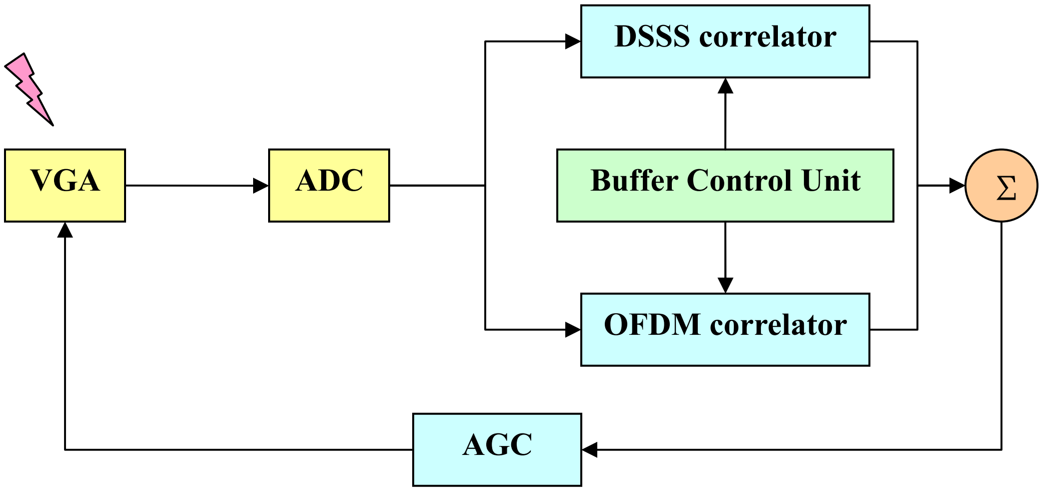

Figure 4-9 The block diagram of proposed method with clearing buffer

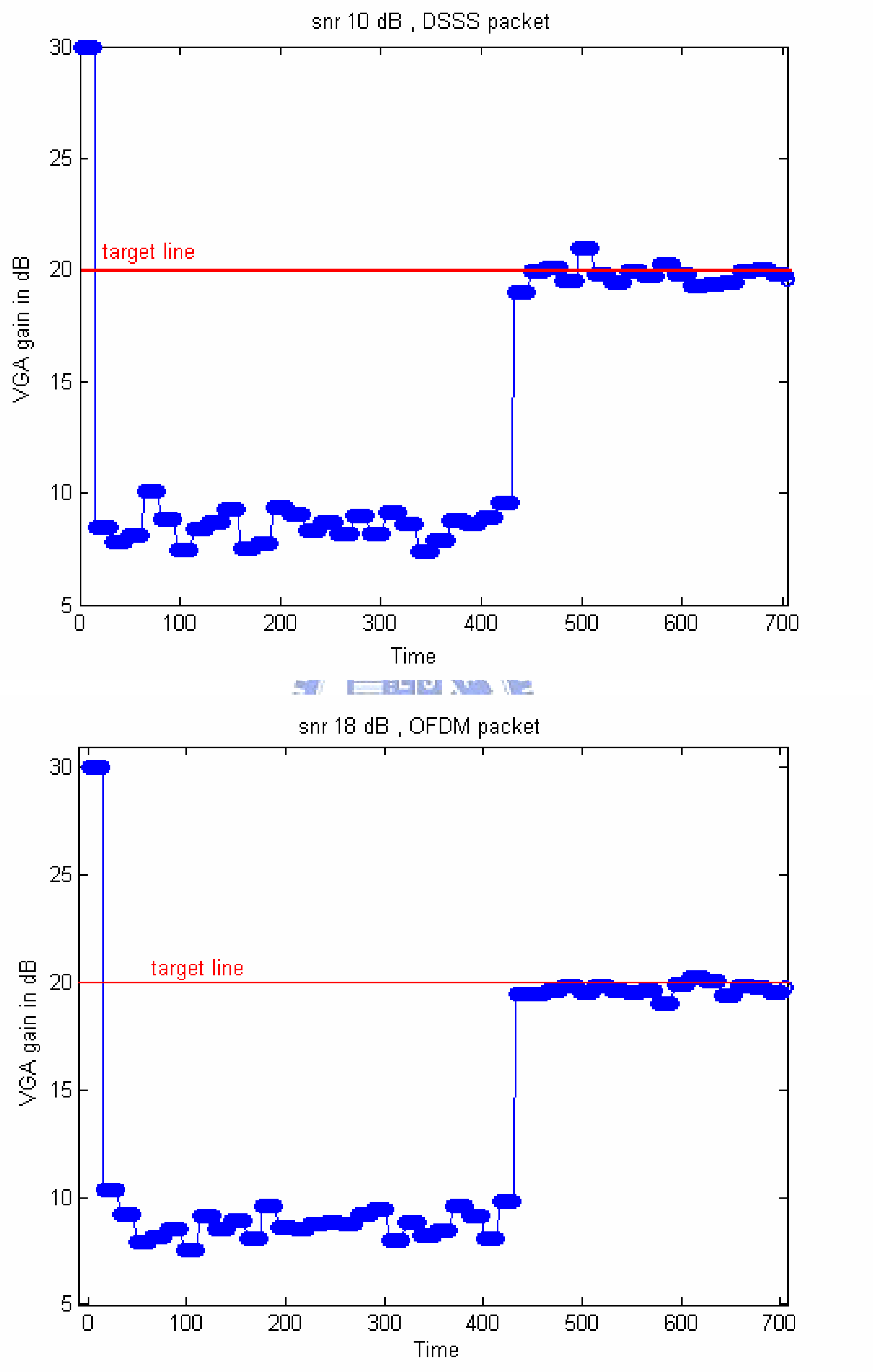

Figure 4-10 VGA gain adjustment at time domain

The VGA gain adjustment of this proposed method at time domain is shown in Figure 4-10. The up side is the situation of transmitting the DSSS type packet and the bottom side is the situation of transmitting the OFDM type packet. Compared with Figure 4-8 and Figure 4-10, it could be found that the method using the sum of correlator output average power of DSSS and OFDM is much more precise than that method using only the sum of sampling point power. Table 4-1 shows the comparison of traditional method and the proposed methods.

Table 4-1 Comparison of traditional AGC and proposed AGC

	Sampling point	Correlator with clearing buffer	Correlator without clearing buffer
Hardware complexity	1 adder 2 squarer	1 adder 2 squarer	1 adder 2 squarer 1 buffer control unit
Precision	Easy interference by AWGN	Resistance to AWGN	Resistance to AWGN
Convergence speed	2~3 symbols	4~6 symbols	2~3 symbols

4.2 Packet detection

The packet detection mechanism must be acting simultaneously with AGC estimating. First, a kind of value-Peak-to-Average-Power Ratio (PAPR) is introduced, and it can be formulated as

$$PAPR=\frac{Peak\_power}{Average\_power} \quad \text{...}(4\text{-}9)$$

$$=\frac{Max(\mathrm{Re}(r(t-nT)\bullet B)^2+\mathrm{Im}(r(t-nT)\bullet B)^2)}{\dfrac{Sum(\mathrm{Re}(r(t-nT)\bullet B)^2+\mathrm{Im}(r(t-nT)\bullet B)^2)}{k}}$$

There are two kinds of information used to detect packet. One is timing and the other is PAPR. Ideally the timing information means that peak will appear at the same position during every symbol time. However, the peak position will not always be the same under AWGN and multipath. So another information-PAPR is used for detecting packet more precisely. Figure 4-11 to 4-14 show the PAPR information during a packet from SNR -5dB to 10dB. From these figure, a message shows that when the SNR increase, the PAPR information of noise and packet will be separated more clearly. But under badly multipath the PAPR information is also become useless and Figure 4-15 shows this kind of situation. The formula of the packet detection rule that using timing information and PAPR information is

$$m = \begin{cases} m+1 & abs(pre\_peakloc - peakloc) <= T \pm 1 or\ PAPR > level \\ 1 & otherwise \end{cases} \qquad \ldots\ldots\ldots\ldots\ldots\ldots\ldots(4\text{-}10)$$

where m is a constant that defined according to the specification of our system, T is the symbol time, Peak_loc is

$$peak\_loc = t - nT + iT_c \ldots\ldots\ldots\ldots\ldots\ldots\ldots\ldots\ldots\ldots\ldots\ldots\ldots\ldots\ldots\ldots\ldots\ldots\ldots\ldots(4\text{-}11)$$

$$\begin{aligned} when\,&\mathrm{Re}(r(t-nT+iT_c)\bullet B)^2 + \mathrm{Im}(r(t-nT+iT_c)\bullet B)^2 \\ &= Max(\mathrm{Re}(r(t-nT)\bullet B)^2 + \mathrm{Im}(r(t-nT)\bullet B)^2) \end{aligned}$$

and pre_peak_loc is

$$pre\_peak\_loc = t - (n-1)T + i'T_c \ldots\ldots\ldots\ldots\ldots\ldots\ldots\ldots\ldots\ldots\ldots\ldots\ldots\ldots\ldots\ldots(4\text{-}12)$$

$$\begin{aligned} when\,&\mathrm{Re}(r(t-(n-1)T+i'T_c)\bullet B)^2 + \mathrm{Im}(r(t-(n-1)T+i'T_c)\bullet B)^2 \\ &= Max(\mathrm{Re}(r(t-(n-1)T)\bullet B)^2 + \mathrm{Im}(r(t-(n-1)T)\bullet B)^2) \end{aligned}$$

respectively. The proposed rule is if the Peakloc, previous Peakloc and PAPR all meet this rule during m continuous symbol time, and then the coming of a packet will be convinced. The larger m is, the correcting rate of detecting a packet is higher, but the wasted symbols during the preamble field is also larger, so a lot of considerations is needed to define the number m. For example, if m is set to 4 that means when m equals 4, a real packet is convinced that it is coming. In other words if you want to make sure that packet comes or not more precisely, you can set a higher number 5, 6, 7 etc. Figure 4-16 is the packet miss rate using this rule under all multipath channel, and the packet miss rate is not zero under the IEEE Multipath when SNR is over 0dB, because the IEEE Multipath is a badly multipath, it will cause the signal distortion very much. However once the Multipath is bad very much, no matter how high the SNR is, packet miss also still appears. So that is why the packet miss rate is not zero when SNR is higher under the IEEE Multipath channel, but the packet miss rate is zero when SNR is higher under the other two Multipath channels, because IEEE Multipath channel is much badly than the other two Multipath channels.

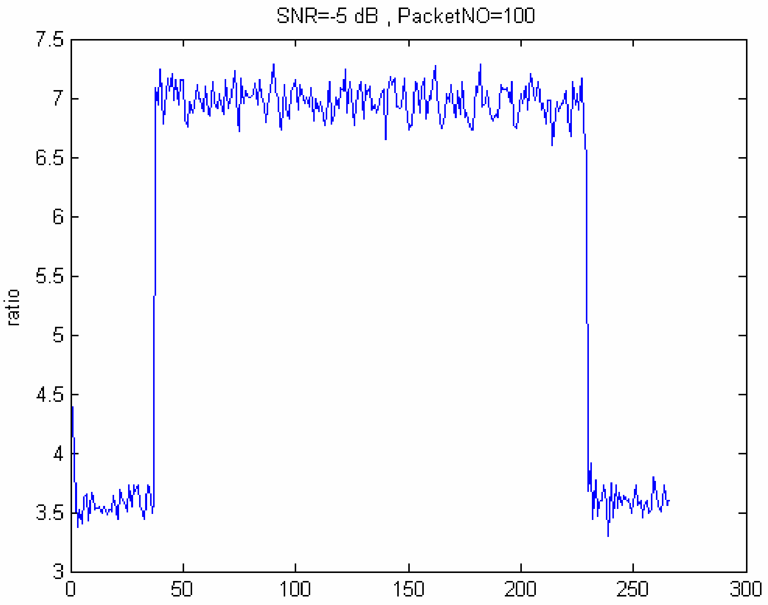

Figure 4-11 PAPR information at SNR -5 dB

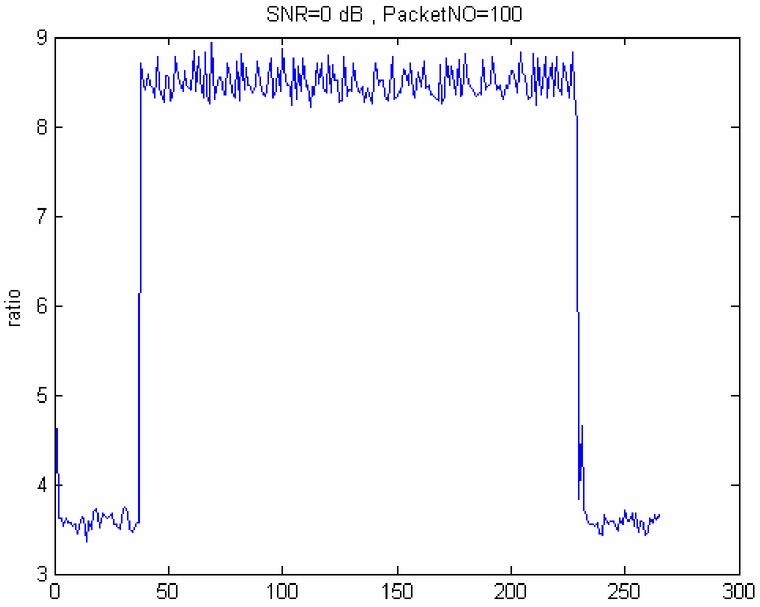

Figure 4-12 PAPR information at SNR 0 dB

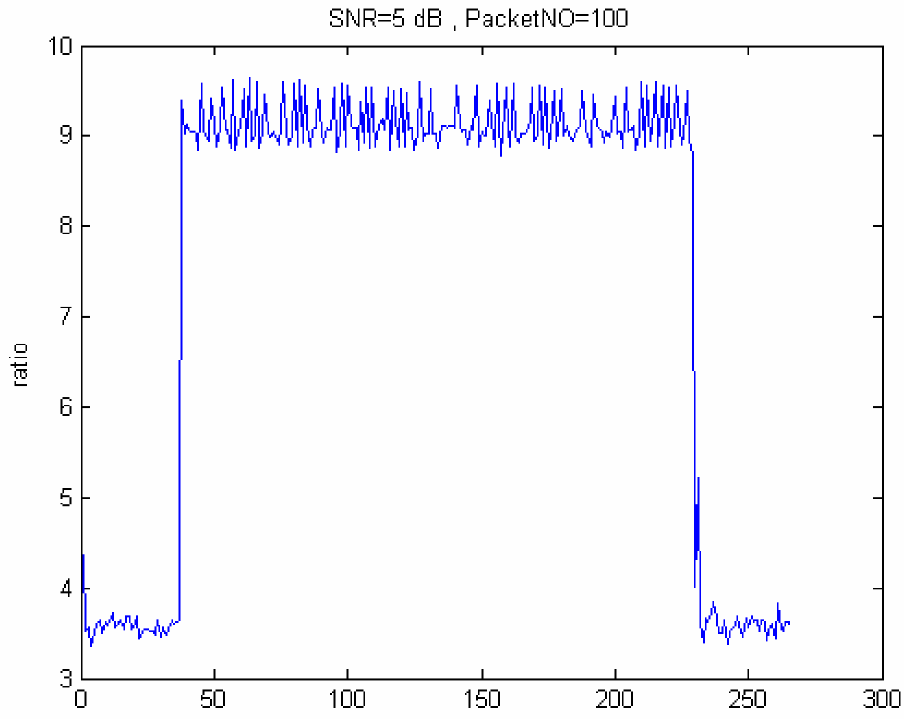

Figure 4-13 PAPR information at SNR 5 dB

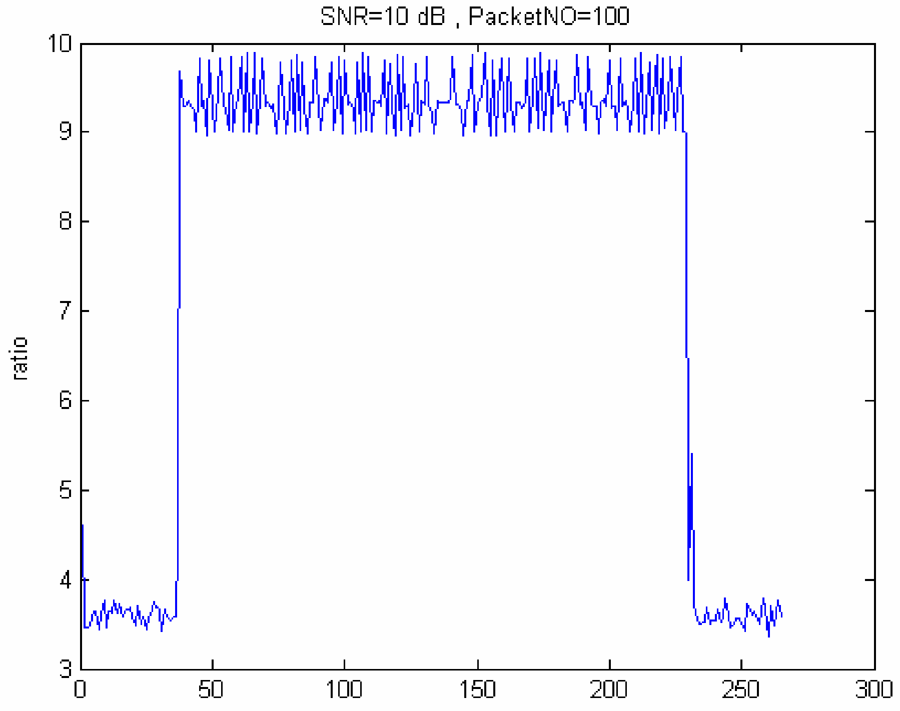

Figure 4-14 PAPR information at SNR 10 dB

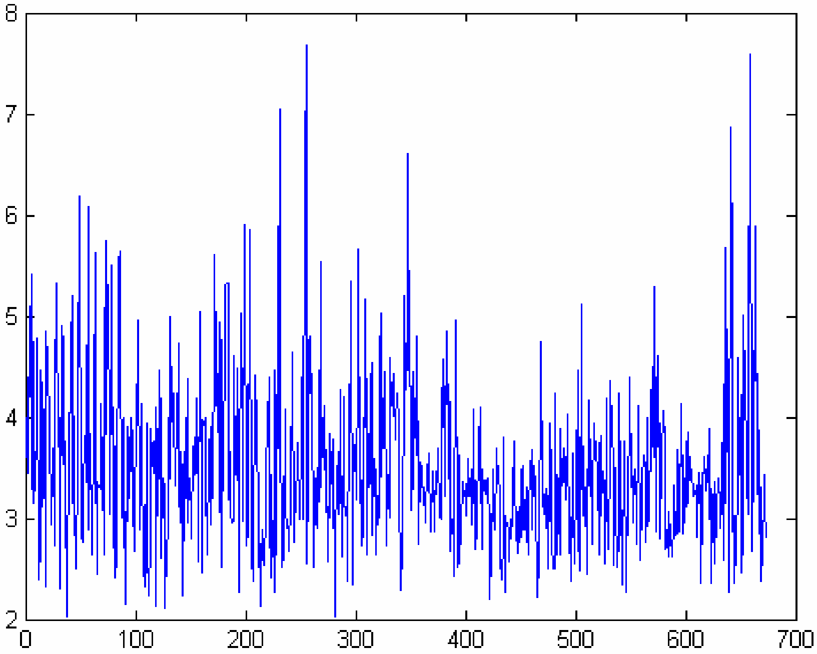

Figure 4-15 PAPR information at SNR 0 dB with IEEE Multipath

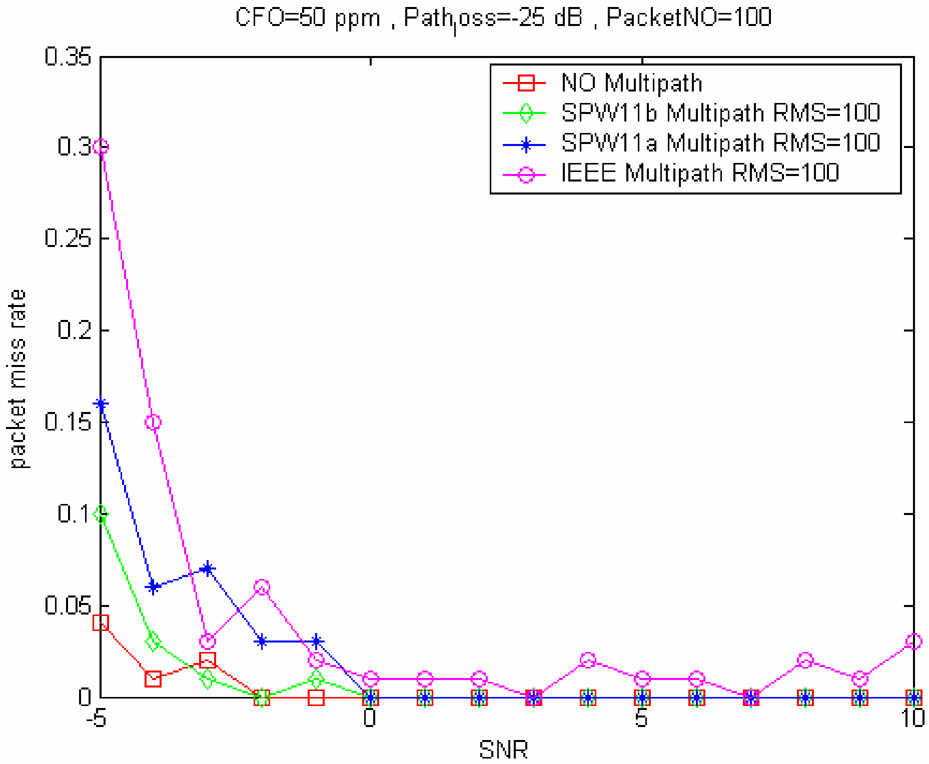

Figure 4-16 Packet miss rate under three Multipath channel

4.3 Symbol boundary decision

After a packet is detected, the symbol boundary is also needed to be decided. Under the situation of only AWGN, if the peak information are used to define the symbol boundary, then the error rate will be the same as usual, because the symbol boundary can always be found at the duration of two continuous peaks. Figure 4-17 shows an example of symbol boundary under the situation of only AWGN, the two solid lines are the symbol boundary defined based on the peak information. However, under the situation of AWGN and badly Multipath, the original peak power may be degraded by Multipath and another power of a point that originally is not a peak may be heightened by Multipath, hence, that may cause a decision of wrong symbol boundary. That situation is shown in Figure 4-18.

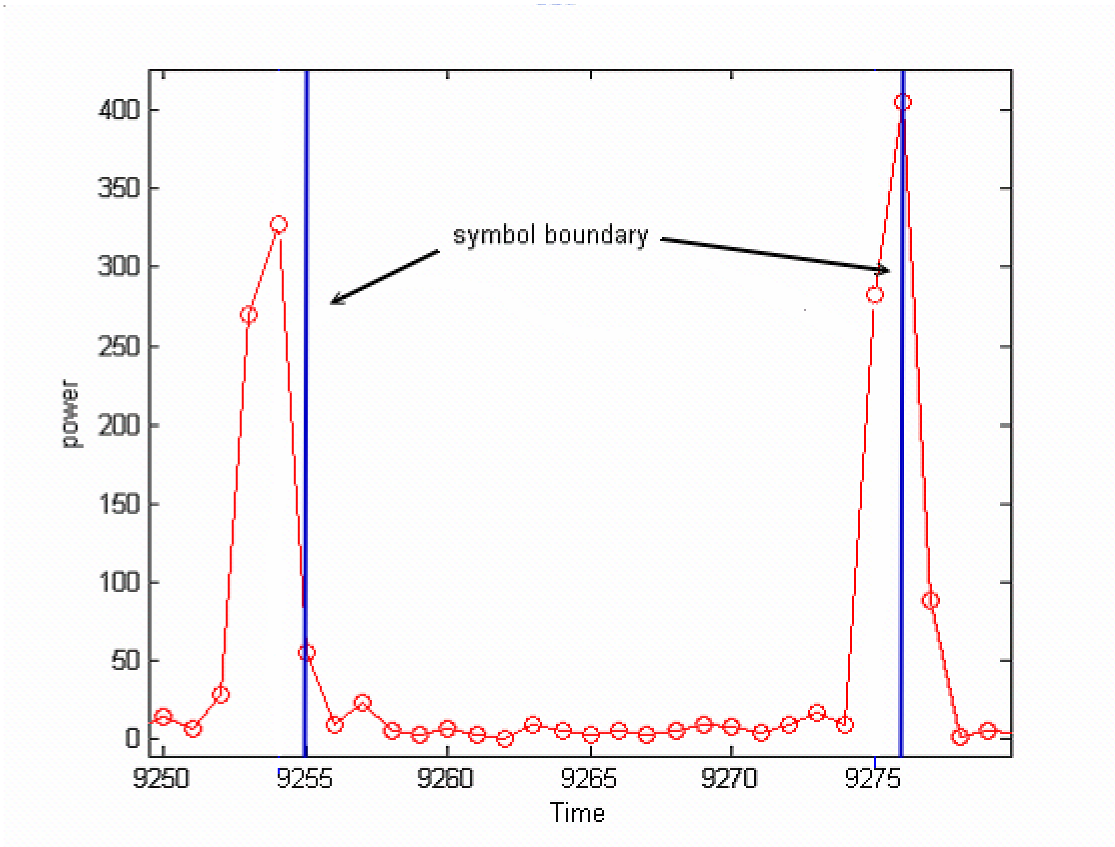

Figure 4-17 Symbol boundary under the situation of only AWGN

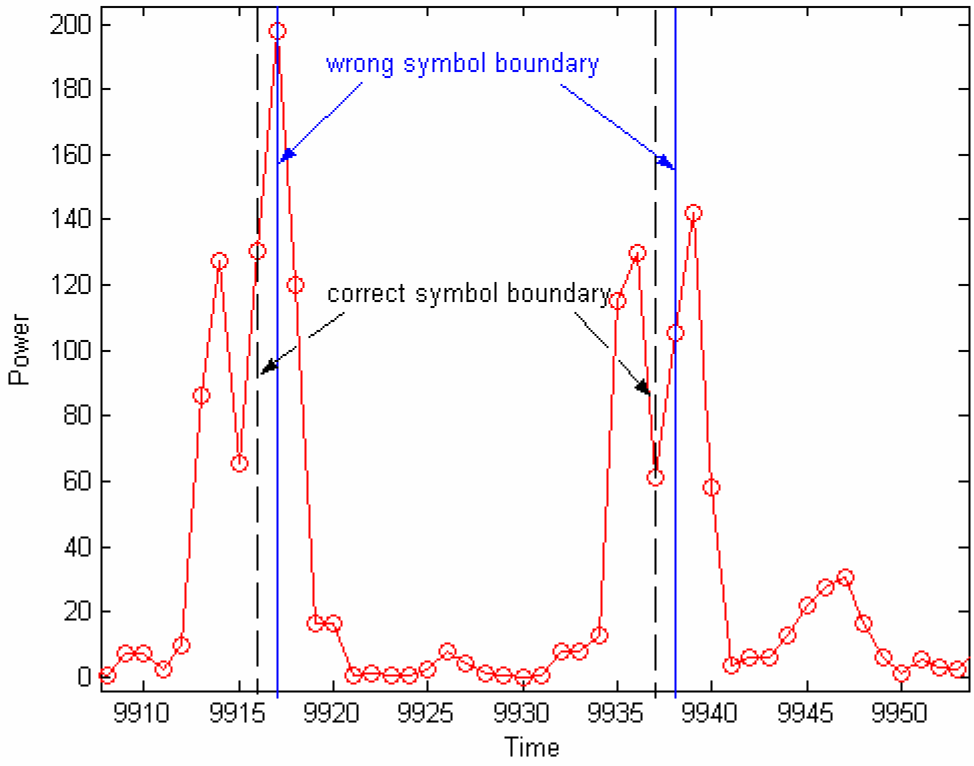

Figure 4-18 Symbol boundary under AWGN and IEEE Multipath

For more correctly deciding the symbol boundary under more complicated channel, the timing information and a new information called pilot that mentioned in previous is used. The pilot is

$pilot = t - nT + i_1 T_c$ ……………………...…………………………..……………..(4-13)

where

$\mathrm{Re}(r(t - nT + i_1 T_c) \bullet B)^2 + \mathrm{Im}(r(t - nT + i_1 T_c) \bullet B)^2 > threshold$

and

$i_1 = \min(\{i_1, i_2, ..., i_p\})$

and the pre_pilot is

$pre\_pilot = t - (n-1)T + i'_1 T_c$ ……………....…………………………….………………..(4-14)

where

$\mathrm{Re}(r(t - (n-1)T + i'_1 T_c) \bullet B)^2 + \mathrm{Im}(r(t - (n-1)T + i'_1 T_c) \bullet B)^2 > threshold$

and

$i'_1 = \min(\{i'_1, i'_2, ..., i'_p\})$

The information of peak_loc and pre_peak_loc are also used here. The proposed symbol boundary rule can be shown in Figure 4-19. the numbers 1, 2, 3, 4 mean the priority that would be chosen to be the symbol boundary. That is there are four results of equations and then the chosen symbol boundary is according to the priority of the decision rule. And the decision rule could be formulated as

$$symbol\_bounday = \begin{cases} peak\_loc & \triangle 1 = \triangle 2 \\ pilot\_loc & \triangle 1 \neq \triangle 2 \ \& \triangle 3 = \triangle 4 \\ peak\_loc & \triangle 1 \neq \triangle 2 \ \& \triangle 3 \neq \triangle 4 \ \& \triangle 1 = \triangle 4 \\ pilot\_loc & \triangle 1 \neq \triangle 2 \ \& \triangle 3 \neq \triangle 4 \ \& \triangle 1 \neq \triangle 4 \ \& \triangle 2 = \triangle 3 \end{cases} \quad \ldots\ldots\ldots\ldots\ldots..(4\text{-}15)$$

$where\ \triangle 1 = peak\_loc,\ \triangle 2 = pre\_peak\_loc,\ \triangle 3 = pilot\_loc,\ \triangle 4 = pre\_pilot\_loc$

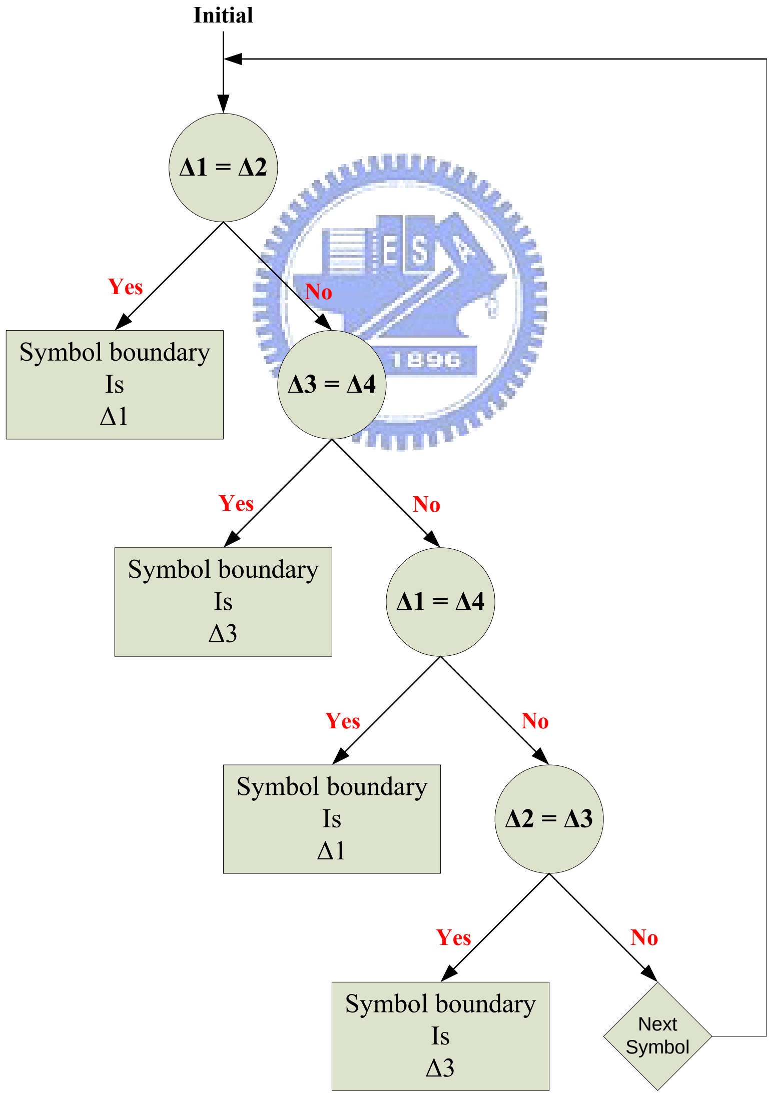

Figure 4-19 The symbol boundary decision rule

Once the symbol boundary is identified, the correlator can be not always busy for producing correlator output, and it just need at the end of one symbol time to get the correlator output, because the symbol boundary has been known. And then the peak_loc also can be known without depending on the correlator output, so the peak power is

$peak\_power$ ……………………………………………………………….…….(4-16)

$$= \mathrm{Re}(r(t-nT+symbol\_boundary \bullet T_c)\bullet B)^2 + \mathrm{Im}(r(t-nT+symbol\_boundary \bullet T_c)\bullet B)^2$$

After the symbol boundary decision, it is the timing synchronization, this component is very important in a wireless communication, but it is no my research topic, it will not be introduce in this thesis.

4.4 Frequency synchronization

4.4.1 CFO introduction

The intention of frequency synchronization is to estimate Δf , the CFO effect between TX and RX in (4-2) and Δf is defined in ppm. The value of Δf in 1 ppm changes with the carrier frequency, for example, with 2.4 GHz carrier frequency, 1 ppm Δf stands for 2.4 kHz offset; however with 5 GHz carrier frequency, 1 ppm Δf stands for 5 kHz offset. The phase offset of rotation of each peak in 1 ppm with 2.4 GHz carrier frequency is

$phase\_offset = carrier\ \ frequency \bullet ppm \bullet time \bullet 360^\circ$ …………………………………(4-17)

$$= 2.4 \bullet 10^9 \bullet 1 \bullet 10^{-6} \bullet 1 \bullet 10^{-6} \bullet 360^\circ$$
$$= 0.864^\circ$$

The max CFO is confined to ± 25 ppm in IEEE 802.11b standard, that is, ± 60 kHz. The max CFO number is different according to different standard. Once CFO occurs badly, the constellation would rotate continuously, and cause the packet error rate (PER) keeps high even when SNR increases. So for keeping the performance well, a CFO estimating and compensating component is needed, hence a Auto Frequency Controller (AFC) is used in our system to play this kind of role. The constellation of received signal through only CFO effect is shown in Figure 3-4. The real part of correlator output with ideal channel and only CFO 25 ppm are shown in Figure 4-20 and Figure 4-21. Compared these two figures, we can see that the peaks on the real part have shape envelope of closing sine or cosine but not very smooth. This situation could be saw in the formula of CFO effect.

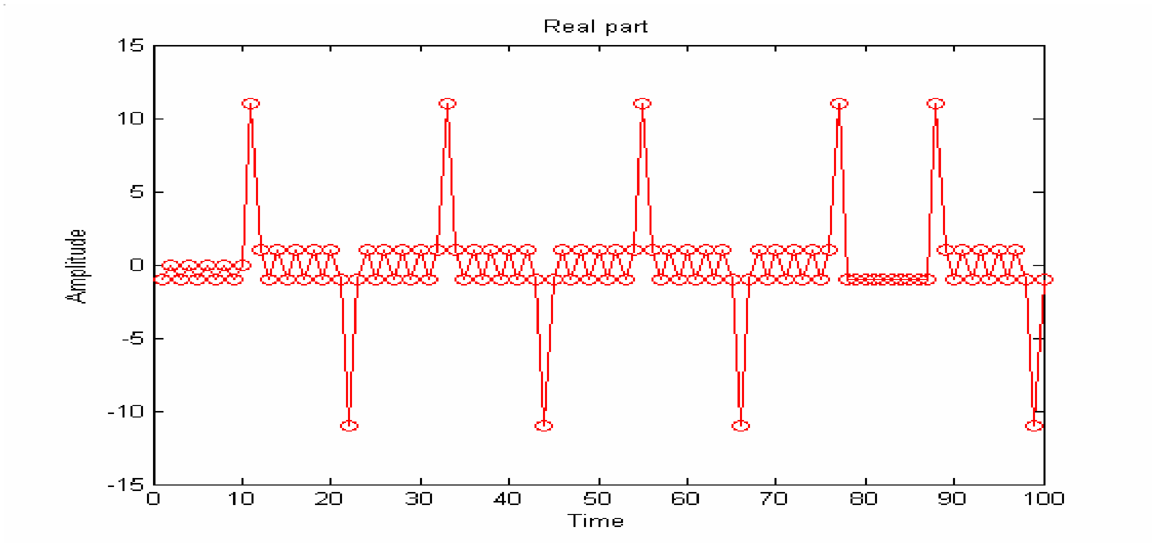

Figure 4-20 Real part of correlator output with ideal channel

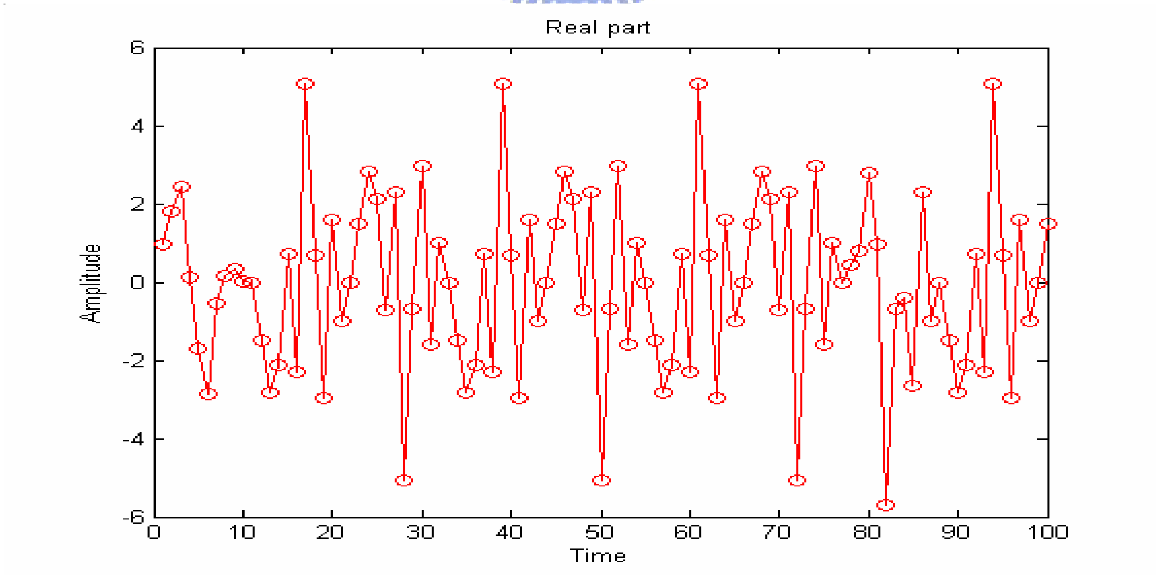

Figure 4-21 Real part of correlator output with CFO 25 ppm

4.4.2 AFC algorithm

In the transmitter passband, the transmitting signal is

$s_p(t) = s(t)\bullet B\bullet e^{j2\pi f_c t}$ ……………………………………………………………….....(4-18)

where f_c is the RF carrier frequency at the transmitter.

and in the receiver passband

$r_p(t) = s_p(t)\bullet e^{-j2\pi f_{c'} t}$ ………………………………………………………………(4-19)

$$\begin{aligned} &= s(t)\bullet B\bullet e^{j2\pi f_c t}\bullet e^{-j2\pi f_{c'} t+\Delta\theta} \\ &= s(t)\bullet B\bullet e^{j2\pi (f_c - f_{c'})t+\Delta\theta} \\ &= s(t)\bullet B\bullet e^{j2\pi\Delta f t+\Delta\theta} \\ &= \mathrm{Re}(s(t)\bullet B)\bullet\cos(2\pi\Delta f t+\Delta\theta)+\mathrm{Im}(s(t)\bullet B)\bullet\sin(2\pi\Delta f t+\Delta\theta) \end{aligned}$$

where $f_{c'}$ is the RF carrier frequency at the receiver, Δf is the CFO and $\Delta\theta$ is the phase offset. The AFC algorithm is proposed to eliminate Δf . The constellation of three consecutive correlator output peaks are shown in Figure 4-22. From this figure, we can see that Δf can be calculated from the phase difference of two consecutive peaks. The phase difference of peak2 and peak3 is bigger than $2\pi\Delta f$, however the actual phase difference is just $2\pi\Delta f$, so two kinds of algorithms can be used to find the actual phase difference. One is that all the peaks are mapping to the right side of Imag axis relative to the origin. If peak3 is mapping to the right side, then the actual phase difference $2\pi\Delta f$ can be correctly calculated. The other method proposed by me is that all peaks do not need be mapping to the right side of Imag axis relative to the origin, a absolute-to-relative phase mapping table is used here and is shown in Figure 4-23. Compared with the first method, the main difference is that the proposed method does not need map peaks at left side of Imag axis to the right side, that is saving a mapping step. The phase of peak$_n$ is

$\theta_n = atr(peak_n)$ …………………………………………………………………...(4-20)

where atr(.) is the absolute-to-relative phase mapping function. The difference phase of two consecutive peaks is

$\theta_n - \theta_{n-1} = \Delta\theta_n = 2\pi\Delta\hat{f}_n T$ ……………………………..………...………………(4-21)

where $\Delta\hat{f}_n$ is estimated and is ready to compensate CFO effect.

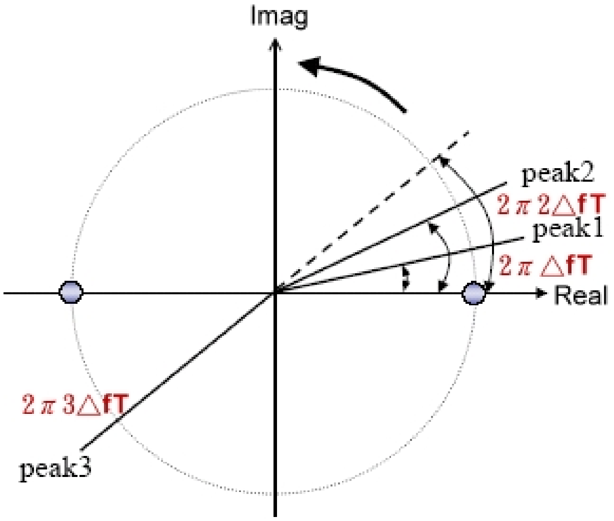

Figure 4-22 Constellation of three consecutive correlator peaks

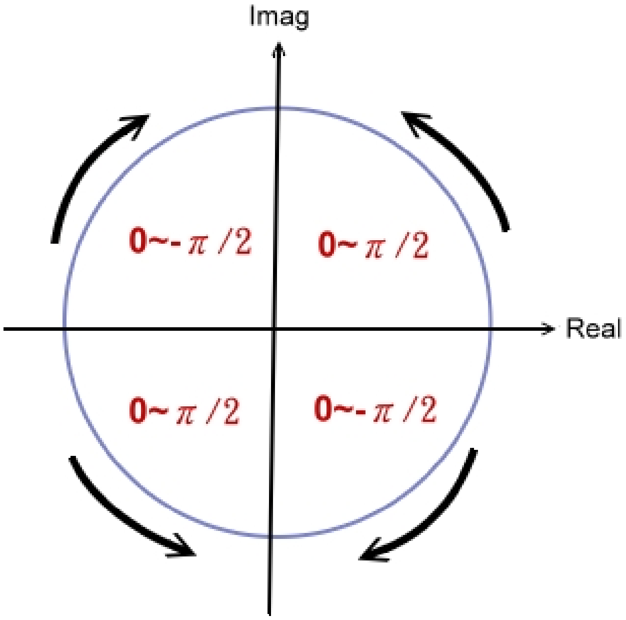

Figure 4-23 Absolute-to-relative phase mapping

And with this proposed method, the CFO could not exceed $\pm 90^\circ$, hence, $\Delta\theta_n$ must be less than $\pm 90^\circ$ and this can be formulated as

$$\Delta\theta_n = \begin{cases} \Delta\theta_n - \pi & when\ \Delta\theta_n > \dfrac{\pi}{2} \\ \Delta\theta_n + \pi & when\ \Delta\theta_n < \dfrac{-\pi}{2} \end{cases} \quad \text{……………………………………………………...(4-22)}$$

For eliminating AWGN effect and better performance, more difference phase of consecutive peaks is used and average them. For example four symbols are taken into average

$$2\pi\Delta\hat{f}T=\frac{(\theta_n-\theta_{n-1})+(\theta_{n-1}-\theta_{n-2})+(\theta_{n-2}-\theta_{n-3})+(\theta_{n-3}-\theta_{n-4})}{4}\cdots\cdots\cdots\tag{4-23}$$

$$=\frac{\Delta\theta_n+\Delta\theta_{n-1}+\Delta\theta_{n-2}+\Delta\theta_{n-3}}{4}$$

$$=\frac{2\pi\Delta\hat{f}_nT+2\pi\Delta f_{n-1}T+2\pi\Delta\hat{f}_{n-2}T+2\pi\Delta f_{n-3}T}{4}$$

$$=2\pi(\frac{\Delta\hat{f}_n+\Delta f_{n-1}+\Delta\hat{f}_{n-2}+\Delta f_{n-3}}{4})T$$

$$\Rightarrow\Delta\hat{f}=(\frac{\Delta\hat{f}_n+\Delta f_{n-1}+\Delta\hat{f}_{n-2}+\Delta f_{n-3}}{4})$$

The estimated angle frequency $-\Delta\hat{f}_n$ is used to compensate CFO, and it will rotate each sample point with this angle frequency. The compensated signal is

$$r_{cfo}(t)=r_p(t)\bullet e^{-j2\pi\Delta\hat{f}t}\cdots\cdots\cdots\tag{4-24}$$

$$=s(t)\bullet B\bullet e^{j2\pi\Delta ft+\Delta\theta}\bullet e^{-j2\pi\Delta\hat{f}t}$$

$$=s(t)\bullet B\bullet e^{j2\pi(\Delta f-\Delta\hat{f})t+\Delta\theta}$$

$$=s(t)\bullet B\bullet e^{j2\pi\Delta\varepsilon t+\Delta\theta}$$

where $\Delta\varepsilon$ is the residual CFO. The step of estimating $\Delta\hat{f}$ is called CFO acquisition. Because $\Delta\varepsilon$ will be very small, $j2\pi(\Delta\varepsilon)t+\Delta\theta$ can be saw as another phase offset $\Delta\theta_\varepsilon$. The phase offset would accumulate phase error as time goes by. So, a step of resetting the phase of NCO after several symbols is called CFO tracking. The formula is

$$r_{cfo}(t)=s(t)\bullet B\bullet e^{j2\pi\Delta\varepsilon t+\Delta\theta}\bullet e^{-\phi}\cdots\cdots\cdots\tag{4-25}$$

$$=s(t)\bullet B\bullet e^{\Delta\theta_\varepsilon-\phi}$$

$$\approx s(t)\bullet B$$

where ϕ is the estimated phase offset at the CFO tracking state after several symbols, and $\Delta\theta_\varepsilon$ is very close to ϕ. Figure 4-24 shows an example of CFO tracking. Figure 4-25 shows the phase at time domain when AFC is on. Figure 4-26 shows the RMSE of CFO range that AFC algorithm can tolerate when SNR is increasing. Figure 4-27 shows the RMSE of CFO acquisition with three Multipath models.

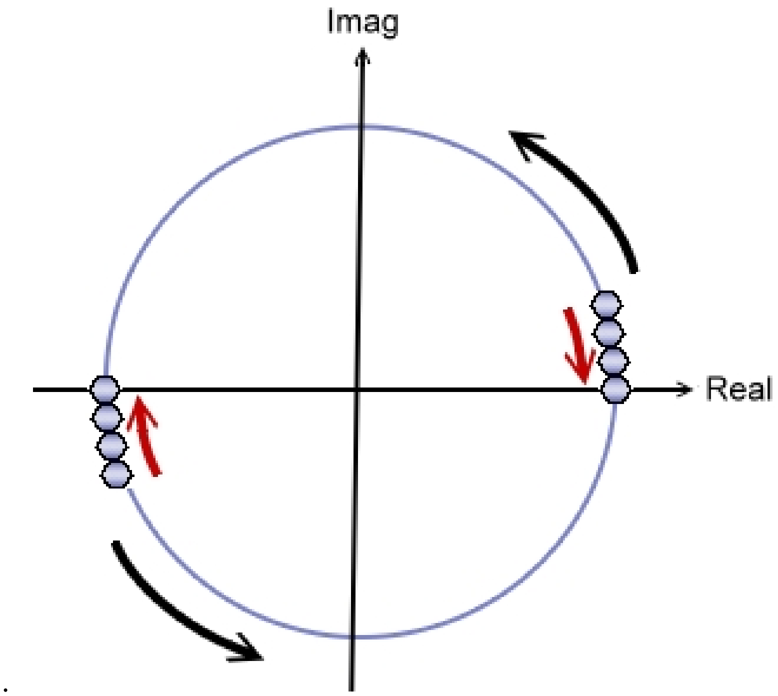

Figure 4-24 Example of CFO tracking

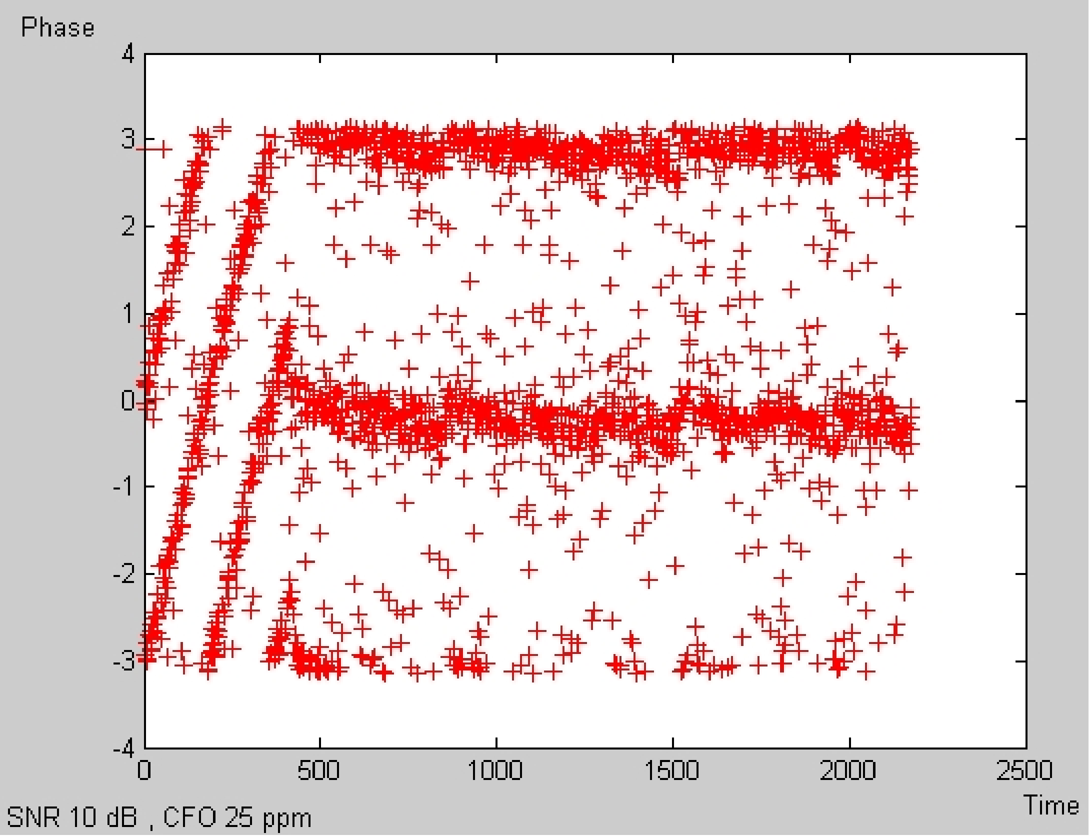

Figure 4-25 Phase of signal at time domain when AFC is on

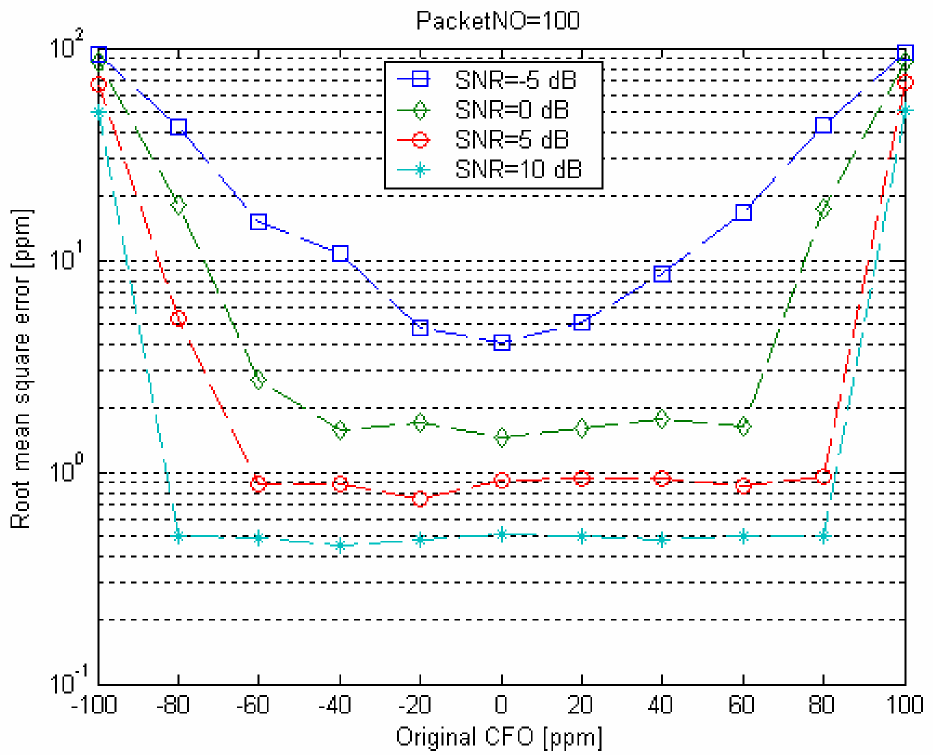

Figure 4-26 RMSE of CFO range that AFC algorithm can tolerate

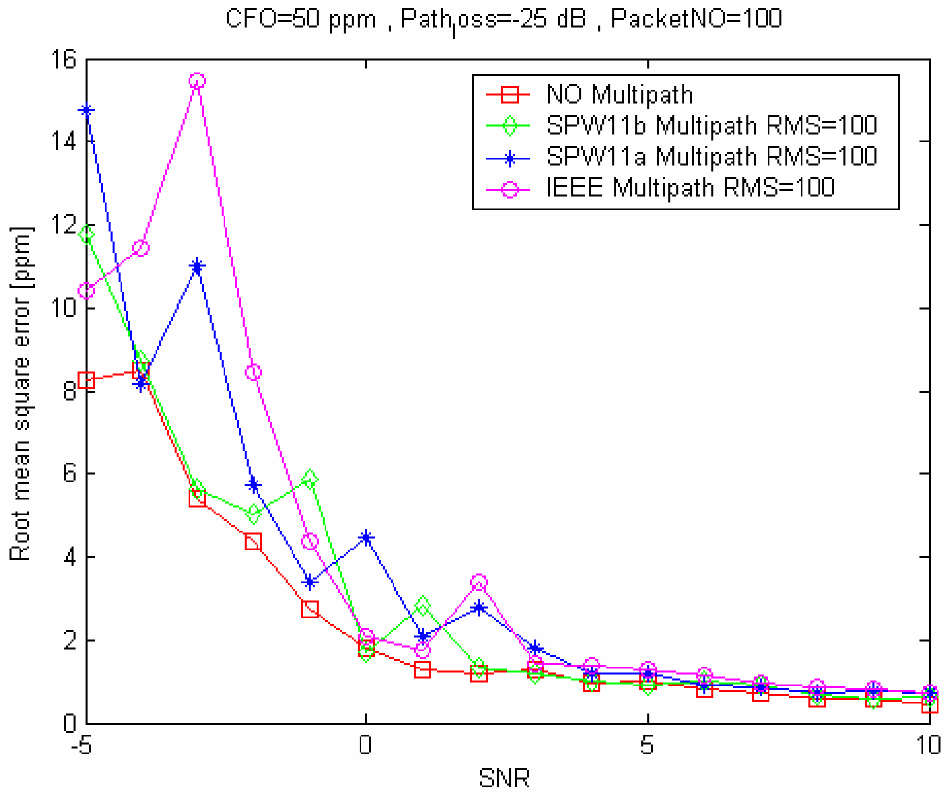

Figure 4-27 RMSE of CFO acquisition with three Multipath models

CHAPTER 5

SIMULATION PLATFORM

5.1 Choosing a suitable tool

The architecture of system platform is shown in Figure 3-6. The initial step that we must care is that choosing a suitable tool – language. Two languages, C/C++ and Matlab are the nice choices, because these two languages have a lot of advantages during the process of constructing platform. These advantages are listed below

a. Complete standard library and document of help

b. Easy to learn programming style

c. High simulation speed

d. Quickly algorithm verification

e. Co-simulate with Verilog

f. Easily porting to HDL

Matlab is chosen as the suitable tool to construct the system platform for the reason of powerful matrix and mathematic functions, friendly Graphical User Interface (GUI), simple debugging tool and many different kinds of figure plotting functions. Although C/C++ has the highest simulation speed, but lack of mathematical functions and less friendly GUI cause us give up it to choose Matlab as the tool. Table 5-1 shows the comparison of C/C++ and Matlab.

Table 5-1 Comparison of C/C++ and Matlab

	Comparison
C/C++	**high simulation speed** **more close to HDL**
Matlab	**friendly GUI** **easy to debug** **powerful matrix operations**

The time that spend on constructing the basic system platform is about two months and the time that spend on algorithm verifying and debugging is about four months. The spending time is less than the expected time, because Matlab give us the most convenience on algorithm level coding and debugging. But more convenience also means that more mapping complexity between algorithm and HDL level. So it needs more experience and more time when Matlab algorithm level is porting to HDL level. Here IEEE 802.11b standard is taken to be the simulation platform, and the PER and BER figures are both produced on this platform.

5.2 System block diagram

Figure 5-1 shows the block diagram of whole system. All important system parameters could be saw in this figure. There three components in this system, transmitter, channel and receiver, and a top file is used to control these three components and call them. The top file controls a parameter-packet number, that parameter defines how many packets the system will execute at the same conditions with increasing SNR.

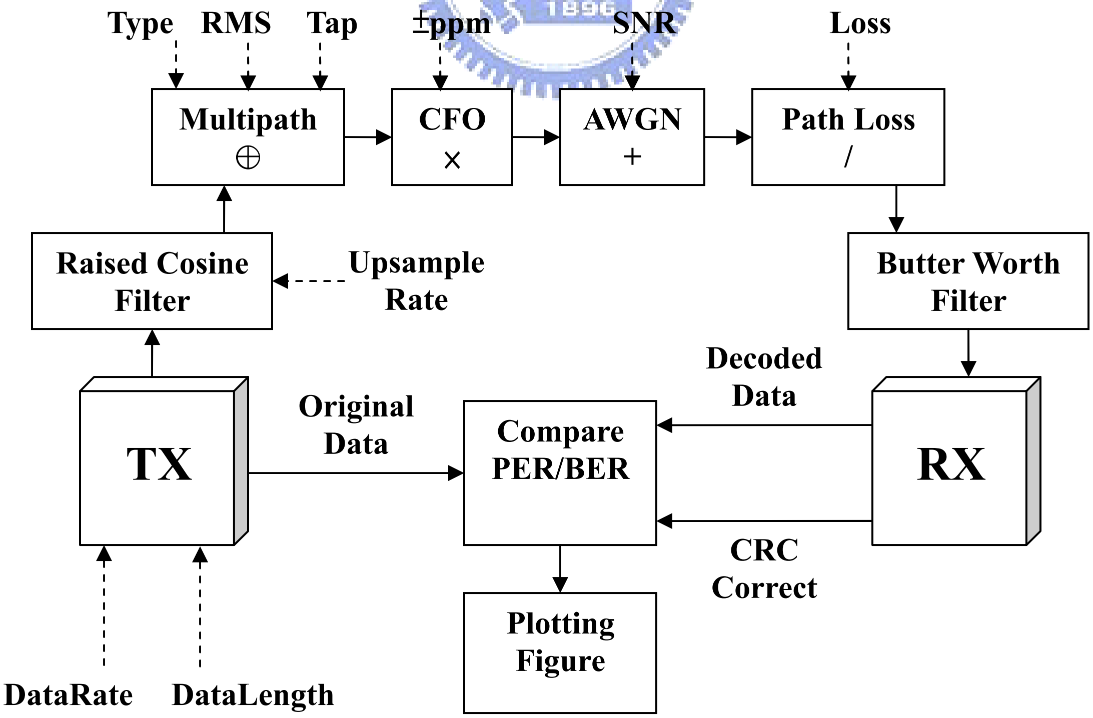

Figure 5-1 System block diagram

5.3 Transmitter

Two parameters control the transmitter component-DataRate and DataLength. The parameter DataRate specifies the signal will be transmitted in which data rate and there are four types of data rate that could be chosen-1 Mbps, 2 Mbps, 5.5 Mbps and 11 Mbps. In 802.11b standard 5.5 Mbps and 11 Mbps are very different to 1 Mbps and 2 Mbps, because data of 5.5 Mbps and 11 Mbps uses CCK code as modulation and spreading code, not like data of 1 Mbps and 2 Mbps uses BPSK, QPSK as modulation and Barker code as spreading code. Although our system can support 5.5 Mbps and 11 Mbps CCK demodulation and decoding, all proposed algorithm focus on DSSS system, so the performance figure PER and BER are both produced at 1 Mbps and 2 Mbps. Figure 5-2 shows the block diagram of transmitter. Because the channel model has been described in chapter 3, we skip it and then describe the details of receiver side.

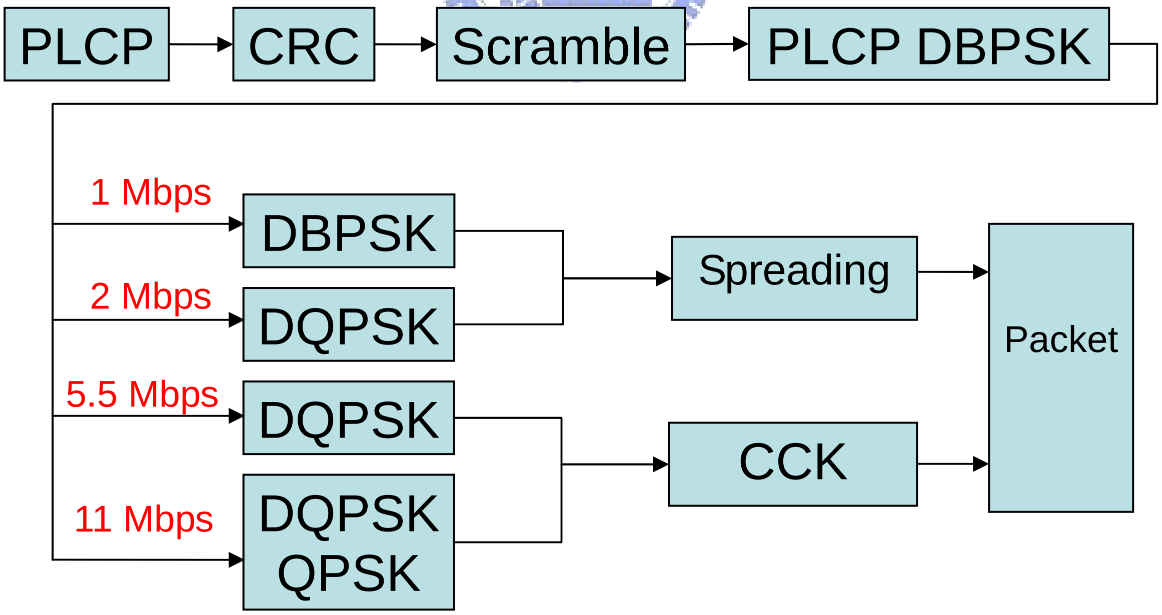

Figure 5-2 Block diagram of transmitter

5.4 Receiver

At the receiver, a finite state machine based coding architecture is used. There are three main advantages listed below

a. Easy to control the process of processing received signal

b. Easily comparing the result between Matlab code and verilog code

c. High extension on adding another components on system

The receiver coding architecture of finite state machine based is shown in figure 5-3. with this kind of coding architecture, we can easy control the flow of processing received signal and anyone can also easy add his algorithm or component to our system. The parameters AGC_on, Timing_on, AFC_on and EQ_on are switches that enable the corresponding components, hence, we can use this kind of coding architecture to simulate the control flow of hardware. For example, the sampled point at this moment will do AGC, AFC and EQ, so the finite state machine just need set AGC_on, AFC_on and EQ_on to 1. Figure 5-4 shows the whole state diagram of receiver. Receiver is the main part of the simulation platform, it contains not only the demodulation function blocks but also the synchronization block which are used to compensate the non-ideal channel effects.

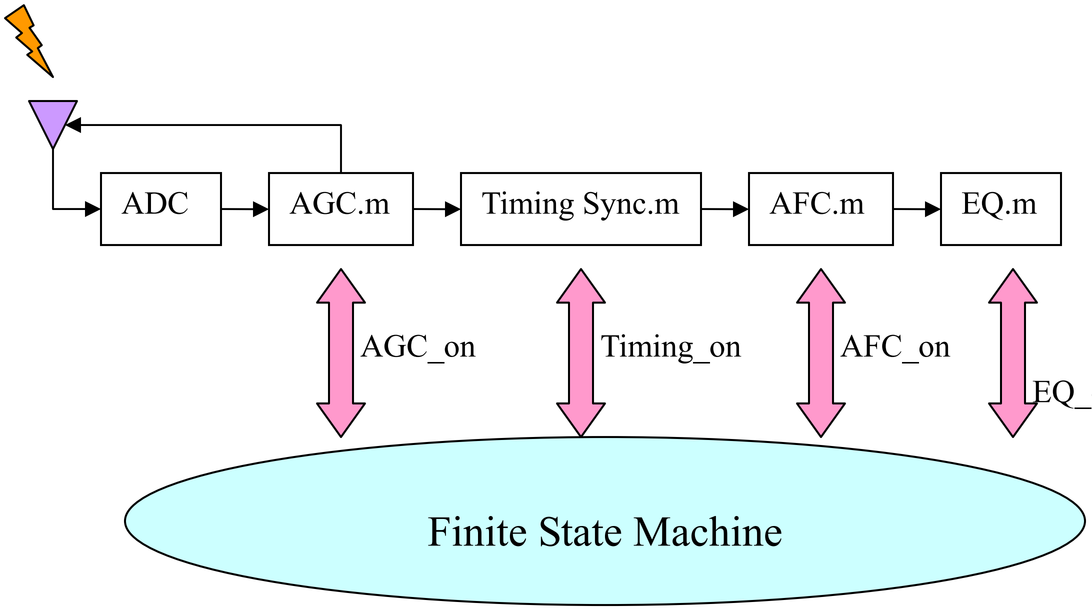

Figure 5-3 Coding architecture of finite state machine based

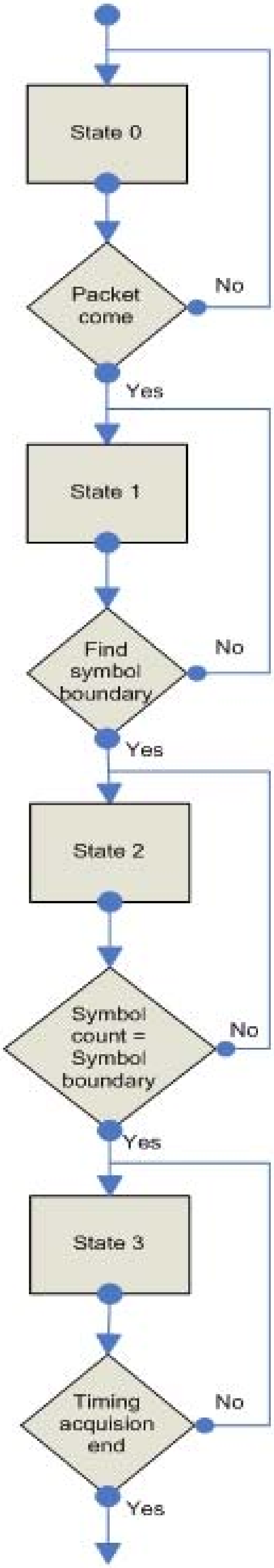
State 0
Packet come
No
Yes
State 1
Find symbol boundary
No
Yes
State 2
Symbol count = Symbol boundary
No
Yes
State 3
Timing acquision end
No
Yes

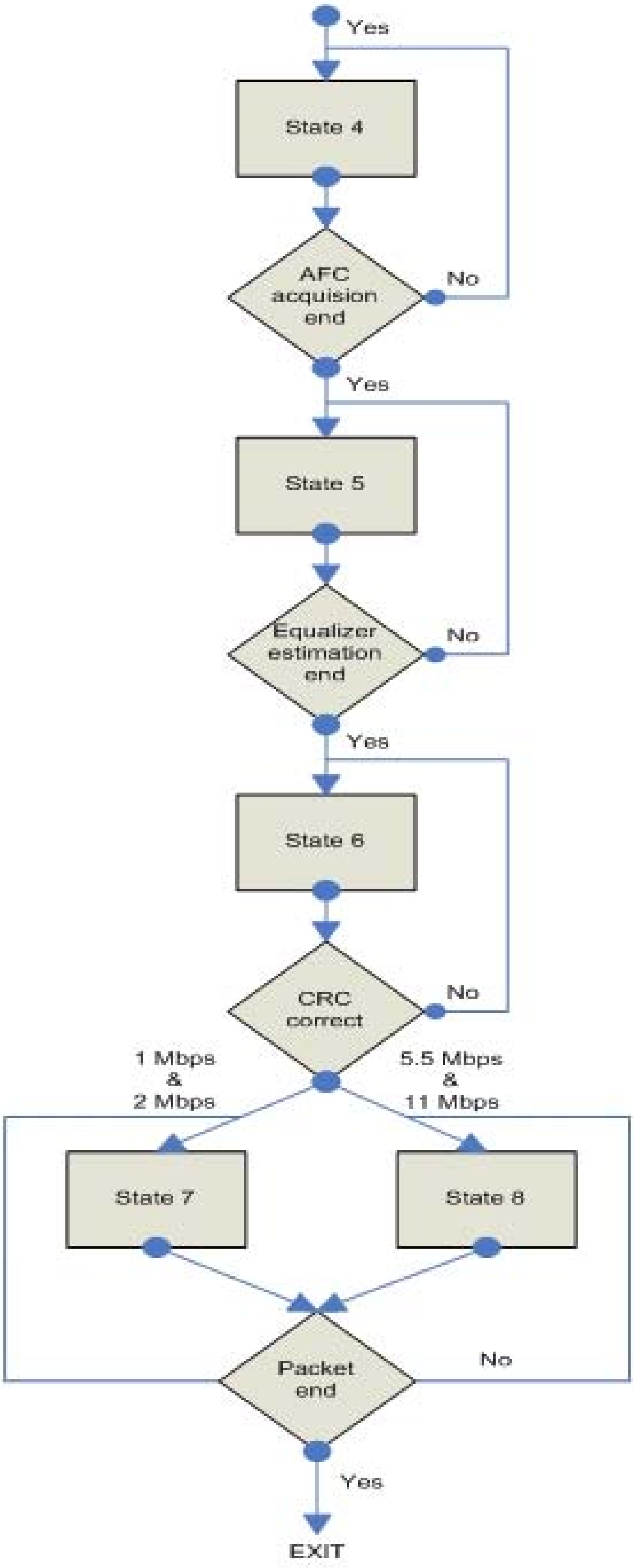

Figure 5-4 State diagram of receiver

5.5 Simulation results

AWGN, multipath, CFO and path loss effects are simulated in our system. To simulate the decision of symbol boundary, random length noise are attached to the head and the tail of the frame as shown in Figure 5-5 when SNR is 10 dB.

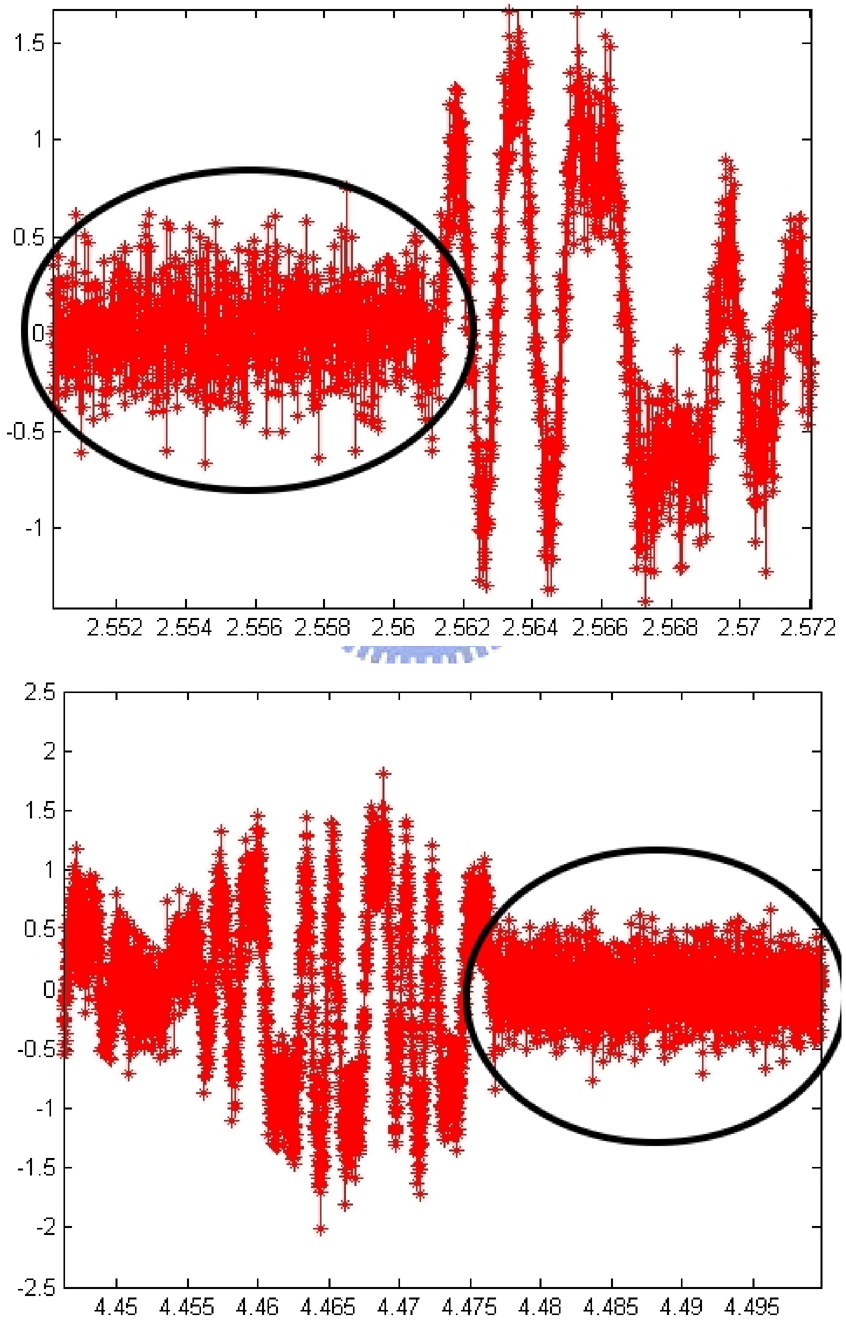

Figure 5-5 Noise attached to the head and tail of the frame

Figure 5-6, 5-7, 5-8 and 5-9 show the PER and BER versus SNR plots. The simulation environment have AWGN, CFO, multipath and path loss. Because all proposed algorithm focus on DSSS, there will on 1 Mbps and 2 Mbps simulation result. The simulation of 5.5 Mbps and 11 Mbps will be skip here, because they are based on CCK and anyone who interested in CCK can refer to thesis[]. All simulation results are simulated with 100 packets, 1024 symbols long, AWGN from -5 dB to 10 dB, CFO 50 ppm and path loss -25 dB. Figure 5-6 shows the PER of 1 Mbps with no multipath and three multipath model.

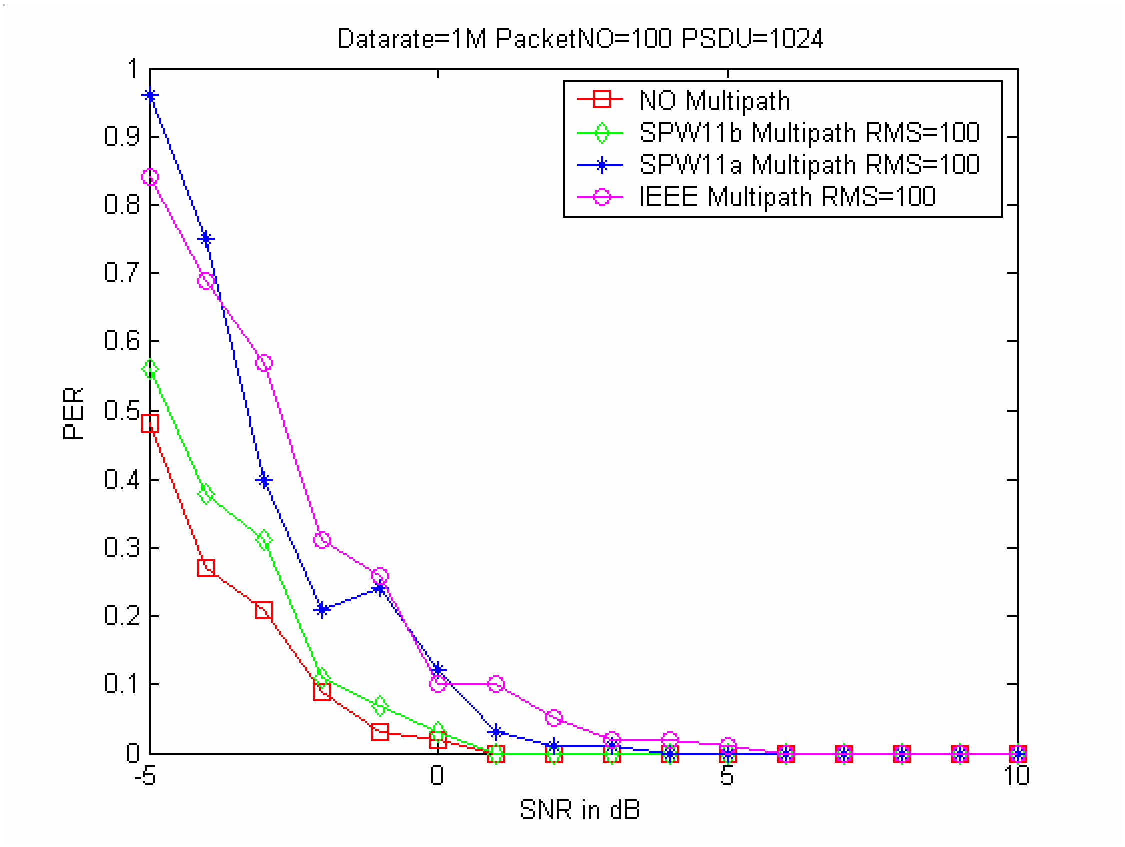

Figure 5-6 PER of 1 Mbps

Figure 5-7 shows the BER of 1 Mbps with no multipath and three multipath model. From Figure 5-6 and 5-7, our system will meet the requirement defined by WiFi at SNR 3 dB with IEEE Multipath model. The WiFi organization defines the requirement of PER and BER are 0.1 and 10^{-5} respectively.

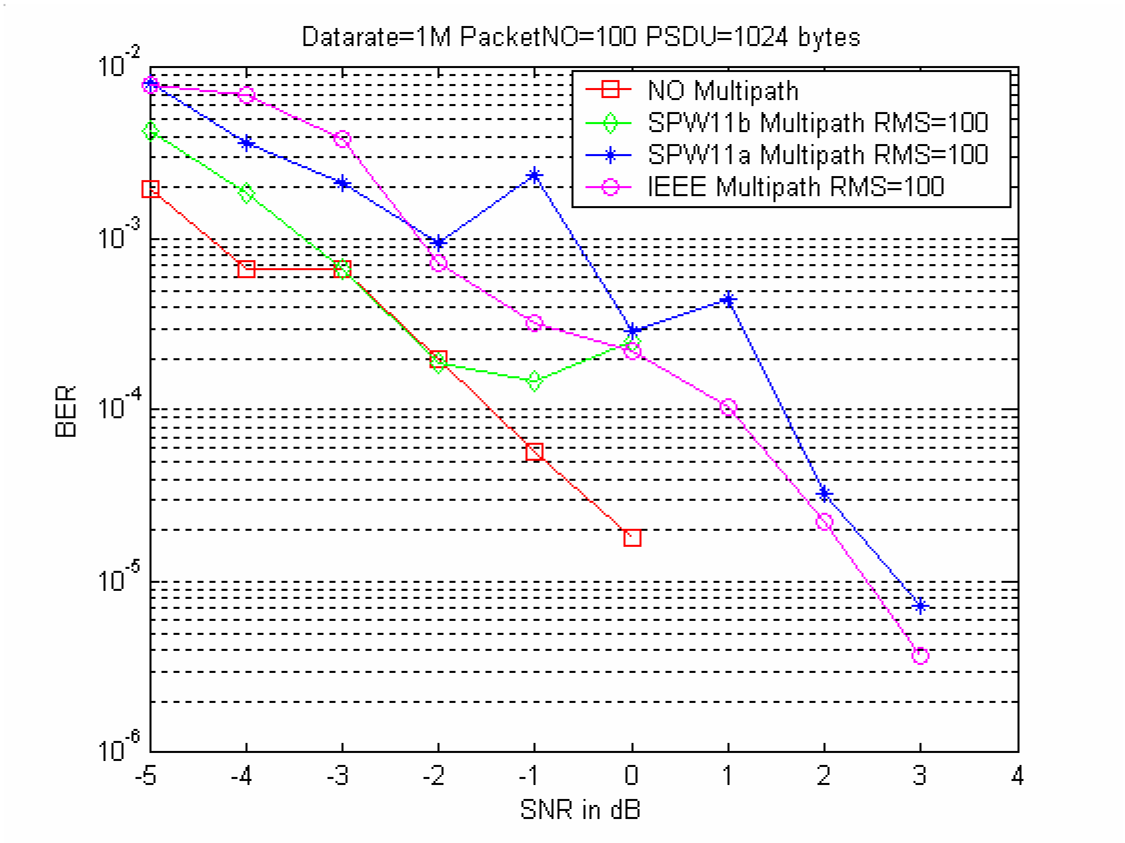

Figure 5-7 BER of 1 Mbps

Figure 5-8 and 5-9 show the PER and BER of 2 Mbps with no multipath and three multipath model respectively. Our system will meet the requirement defined by WiFi at SNR 10 dB with IEEE Multipath model. From these four figures, we can find that the signal with higher data rate will be affected more seriously than the signal with lower data rate.

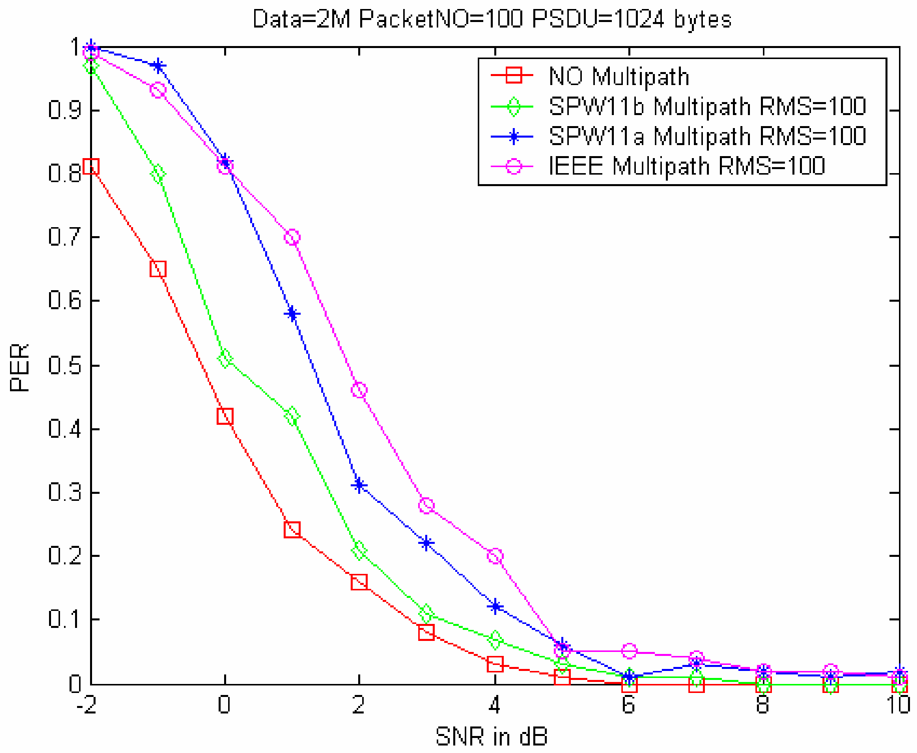

Figure 5-8 PER of 2 Mbps

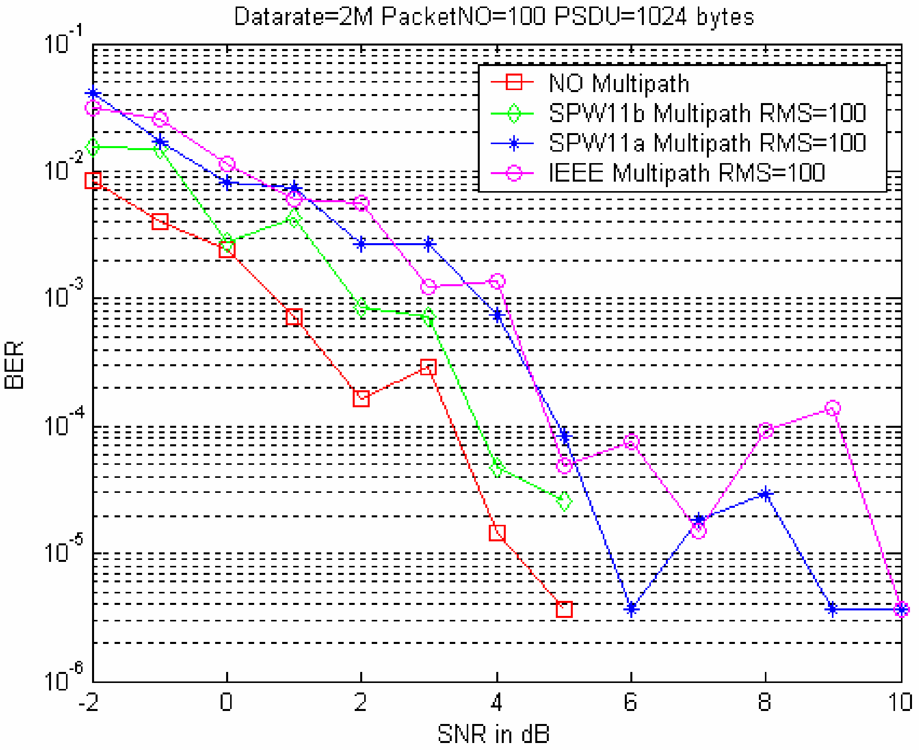

Figure 5-9 BER of 2 Mbps

CHAPTER 6

CONCLUSIONS AND FUTURE WORKS

6.1 Conclusions

The front-end signal process and frequency synchronization algorithms were proposed for DSSS based wireless baseband applications. For deeply verifying these proposed algorithms do not affect the data decoding and whole system performance. So the IEEE 802.11b system is used to combine with our proposed algorithms. From the BER and PER of 1 Mbps and 2 Mbps, the proposed algorithms do not seem to affect the process of data decoding and demodulation. With our proposed algorithms, these could be used on any other wireless communications for DSSS based, like DSSS UWB system and sensor network system, etc. The proposed algorithms seem to could against multipath fading with signal of lower data rate like 1 Mbps and 2 Mbps. My another contribution is that constructing a confident and easily usable simulation platform to let other teammates verify their algorithms respectively, like timing synchronization algorithm, channel estimation and compensation algorithms of equalizer. The contributions of team work are much greater than contributions of oneself work, because our goal is to establish a DSSS based system at frequency domain for sharing a lot of components with OFDM based system, like IEEE 802.11g.

6.2 Future works

For implementing a chip finally, the fixed-point simulation is needed. So, the current floating-point (algorithm level) platform must been changed to fixed-point platform. During the process of constructing a fixed-point platform, many considerations must be concerned, for example, what the number of bits of ADC is, how to decide the number of bits after each operation, how to make a Look-Up-Table (LUT) for mapping and what size the LUT is, etc. A lot of time is needed for fixed-point platform constructing and simulating. A more flexible AGC algorithm for dual system and more complicated channel is needed. Because for higher speed wireless communication system, Doppler effect will dominate the performance of whole system. Hence, a more deeply research on the power decade with Doppler effect is needed. And for more complicated channel, the path loss effect will not usually be a constant, it will decrease a little during a period of time, hence a more flexible AGC algorithm must handle this situation. I will learn more knowledge and do research more harder in my future work.

References

[1] "Wireless LAN Medium Access Control (MAC) and Physical Layer (PHY)", specifications, IEEE 802.11b standard 1999

[2] "Wireless LAN Medium Access Control (MAC) and Physical Layer (PHY)", specifications, IEEE 802.11a standard 1999

[3] "Wireless LAN Medium Access Control (MAC) and Physical Layer (PHY)", specifications, IEEE 802.11g standard 2003

[4] Chien-Jen Hung, "A Differenctial Decoding Based Baseband Processor for DSSS Wireless LAN Applications", NCTU, master thesis, June 2003

[5] Bernard Sklar, Digital Communications - Fundamentals and Applications Second Edition, Prentice-Hall Inc., Communication Engineering Services, Tarzana, California and University of California, Los Angeles, 2001

[6] A. L. Welti, B. Z. Bobrovsky *, "Doppler Acceleration Influence On Code Tracking In Direct Sequence Spread Spectrum Systems: Threshold Calculation And AGC Algorithms", Global Telecommunications Conference, IEEE, 1624 - 1628 vol.3, Dallas, TX USA, Nov. 1989

[7] T. Drenski, L. Desclos, M. Madihian, H. Yoshida, H. Suzuki, T. Yamazaki, "A BiCMOS 300ns Attack-Time AGC Amplifier with Peak-Detect and Hold Feature for High-Speed Wireless ATM Systems", Solid-State Circuits Conference, ISSCC, IEEE International, p. 166-167, San Francisco, CA USA, Feb. 1999

[8] Peter Kreuzgruber, "A Class of Binary FSK Direct Conversion Receivers", Vehicular Technology Conference, IEEE, 457 - 461 vol.1, Stockholm Sweden, 1994

[9] Arnold L. Welti, Member, IEEE, and Ben-Zion Bobrovsky, Member, IEEE, "On Optimal AGC Structure for Direct Sequence Spread Spectrum PN-Code Tracking"

[10] Mitsuhiko YAGYU, Shigenori KINJO and Hirohisa YAMAGUCHI, Texas Instruments Tsukuba R&D Center, "Analysis and Minimization of Loss of Process Gain with A/D Conversion in DS-CDMA", Vehicular Technology Conference, IEEE VTS, 2476 - 2480 vol.5, Amsterdam Netherlands, 1999

[11] Won Namgoong, "ADC and AGC Requirements of A Direct-Sequence Spread Spectrum Signal", IEEE 2001 Midwest Symposium on Circuits and Systems, 744 -

747 vol.2, Dayton, OH USA, 2001

[12] Miaochen Wu, Xiangdong Zhang, Angelos Alexanian, Wei Ye, “Analog Baseband Receiver Chip for 100 Mbps/1Gbps Broadband Symmetric Cable Modem”, Bipolar/BiCMOS Circuits and Technology Meeting, p. 185-188, 2002

[13] M. Luise, R. Reggiannini, “Carrier Frequency Recovery in All-Digital Modems for Burst-Mode Transmissions”, IEEE Trans. Commun., COM-43, 1169-1178, 1995

[14] D. G. Messerschmitt, “Frequency Detectors for PLL Acquisition in Timing and Carrier Recovery”, IEEE Trans. Commun., COM-27, 1288-1295, Sept. 1979.

[15] Magill D.T., Personal, "A Fully-integrated, Digital, Direct sequence, Spread spectrum modem ASIC”, IEEE International Symposium on Indoor and Mobile Radio Communications, p. 42-46, Oct. 1992

[16] Fawer U., “A Coherent Spread-spectrum Diversity-receiver with AFC for Multipath Fading Channels”, IEEE Transactions on Communications , p. 1300-1311, Volume: 42 , Issue: 234 , April 1994

[17] Saarnisaari H. “An Approximative Maximum Likelihood Frequency Detector for DS/SS Systems”, IEEE International Symposium on Spread Spectrum Techniques and Applications, 747-750 vol. 2, Sept. 2000

[18] Jing Lei, Tung-Sang Ng, “A Non-data-aided and Non-phase-based AFC method for MPSK DS/CDMA Transceivers Used in Digital Broadcasting”, IEEE Transactions on Broadcasting, 335-343, vol. 49 , Issue: 4, Dec. 2003

[19] Theodore S. Rapaport, Wireless Communications – Principles and Practice, Prentice Hall, 1996

[20] W. C. Lindsey, M. K. Simon, Englewood Cliffs, Telecommunication Systems Engineering, Prentice Hall, 1972

[21] http://www.wi-fi.org/

[22] http://intel.com/

[23] http://www.intersil.com/

[24] http://www.ti.com/

[26] http://www.agere.com/

About the Author

LO SHIH LIN, male, was born in Taipei County, Taiwan (R.O.C.), on January 22th, 1980. He received the B.S degree in computer science from National Tsing Hua University (NTHU) in June 2002 and make efforts in master degree at Nation Chiao Tung University from September 2002. His research focuses on wireless communication systems, especially on WLAN. In the two years of graduate, he learned a lot of theoretical and practical courses, like Wireless LAN, Personal Communication System (PCS), Algorithm, Computer Architecture, Digital Communications, IC Design LAB(1)(2), Embedded Operating System and Network Programming. These courses give a huge help on his research and master thesis. The title of his master thesis is "The Study of Front-End Signal Process for Wireless Baseband Applications".